

Synthetic Methods

General Considerations. Unless otherwise specified, all manipulations were performed under an inert atmosphere by standard Schlenk techniques or in an M. Braun Unilab N₂-filled glove box maintained at or below 1 ppm of O₂ and H₂O. Glassware was dried at 150 °C overnight. ¹H NMR and ¹³C NMR spectra were recorded on a Bruker Avance 500 MHz spectrometer at room temperature. Shifts (δ) are reported in ppm, relative to residual protiated solvent in C₆D₆ (δ 7.15 ppm, 128.06 ppm), CDCl₃ (δ 7.26 ppm, 77.23 ppm) or THF-d₈ (δ 1.73, 3.58 ppm). Peaks were singlets unless otherwise noted. Solution magnetic susceptibilities were determined by Evans' method.^{1,2} NMR assignments are based on the labels shown in Figure S-1.

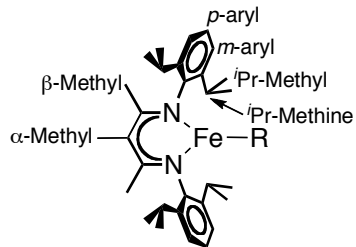


Figure S-1. A general iron complex with the β -diketiminate ligand (^{Me}L^{Me}) labeled to clarify NMR assignments below.

Pentane, diethyl ether, THF (tetrahydrofuran) and toluene were purified by passage through activated alumina and “deoxygenizer” columns from Glass Contour Co. (Laguna Beach, CA). THF was further dried by distilling from Na/benzophenone. Deuterated benzene was first dried over activated alumina and then filtered before use. THF-d₈ was dried over CaH₂ and then

over Na/benzophenone and vacuum transferred to a storage container before use. Celite was dried at 200 °C under vacuum overnight.

Infrared data were obtained on a Shimadzu FT-IR 8400S spectrometer using KBr pellets or as a neat solid. Frequencies are given in cm^{-1} . Electrochemical data were obtained using a Cypress Systems 3100 potentiostat. The working electrode was glassy carbon with a 1 mm diameter working area and Ag wires were used as auxiliary and reference electrodes. All spectra were taken using a 50 mM $[\text{NBu}_4][\text{BAr}^F_4]$ ($\text{Ar}^F = 3,5\text{-bis-(CF}_3\text{Ph)}_4\text{B}$) electrolyte solution in Et_2O or THF. The scan rate was 200 mV/s unless otherwise noted. Differential pulse experiments used a sweep width height of 500 mV, step height of 2 or 4 mV and a sweep width period of 20 mS. All measurements were referenced to the $\text{Cp}_2\text{Fe}^+/\text{Cp}_2\text{Fe}$ couple using an internal ferrocene standard. Electronic spectra were recorded between 400 and 1000 nm on a Cary 50 UV-visible spectrophotometer, using airfree cuvettes of 0.1 cm optical path length. Extinction coefficients are given in $\text{mM}^{-1} \text{cm}^{-1}$. Elemental analyses were performed by University of Illinois (Urbana, Illinois) or Columbia Analytical Services (Tucson, AZ) and the CENTC Elemental Analysis Facility at the University of Rochester. Mass spectrometry analyses used electrospray ionization, and were done on a Shimadzu QP2010 LCMS.

KC_8 was prepared by heating potassium and graphite at 150 °C under an argon atmosphere. Benzylpotassium was made using a published synthesis.³ HL^{Me} was synthesized using a published method^{4,5} followed by deprotonation with benzylpotassium³ in Et_2O . $\text{FeCl}_2(\text{THF})_{1.5}$ was made as previously published.⁶ $\text{L}^{\text{Me}}\text{Fe}^{\text{i}}\text{Bu}$ was also synthesized through a published procedure.⁷ Me_3PS was synthesized using a modified published synthesis in which

PMe_3 was stirred with 1/8 molar equivalents of S_8 in toluene for 12 hours.⁸ $\text{Na}[\text{BAr}^{\text{F}}_4]^9$ was made using a published procedure.^{9,10} KOTf ($\text{OTf} = \text{CF}_3\text{SO}_3^-$) was purchased from Aldrich and dried at 100 °C under vacuum overnight before use.

$\text{H}^{\text{Me}}\text{L}^{\text{Me}}$. Under an N_2 atmosphere, MeI (3.6 mL, 57.7 mmol) was added by syringe to a cooled yellow solution (-78 °C) of KL^{Me} (24.0 g, 52.5 mmol) in Et_2O (70 mL). The solution was warmed to room temperature over 1 hour and it turned cloudy and white. The mixture was stirred at room temperature for 1 hour and then exposed to air and dried under vacuum. The light-yellow product was extracted using Et_2O (3 x 50 mL) from water (50 mL) and dried over MgSO_4 . The solution was put under vacuum until it became a tan oil. In the glove box, the oil was redissolved in dry Et_2O (80 mL) and stored over activated 4 Å molecular sieves (3 x 12 hrs). The solution was concentrated to 60 mL and cooled to -35 °C to give a white solid (17.8 g, 41.0 mmol, 78%). The kinetic product was the diimine tautomer and significant conversion to the thermodynamic product, the enamine/imine tautomer, was seen in about a week when left out in air. **Diimine tautomer:** ^1H NMR (500 MHz, CDCl_3) δ 7.3 (d, 4H, *m*-aryl), 7.2 (t, 2H, *p*-aryl), 3.9 (q, $J = 7$ Hz, 1H, α -H), 2.8 (sept., $J = 7$ Hz, 4H, *i*Pr-methine), 1.9 (s, 6H, β -methyl), 1.7 (d, $J = 7$ Hz, 3H, α -methyl), 1.3 (2x overlapping doublet, 24H, *i*Pr-methyl) ppm. ^{13}C NMR (500 MHz, CDCl_3) δ 171.3 (β -C), 146.3 (*i*-C), 136.4 (*o*-C), 123.6 (*p*-Ar), 123.2 (*m*-C), 123.1 (*m*-C), 56.0 (α -C), 28.2 (*i*Pr-CH), 28.1 (*i*Pr-CH), 23.7 (*i*Pr-methyl), 23.5 (*i*Pr-methyl), 23.3 (*i*Pr-methyl), 23.2 (*i*Pr-methyl), 19.3 (β -methyl), 15.7 (α -methyl) ppm. MS (El^+): *m/z* (relative intensity): 433 (100%), 434 (32%), 435 (6%). Anal. Calcd for $\text{C}_{30}\text{H}_{44}\text{N}_2$: C, 83.28, H, 10.25, N, 6.47. Found: C, 83.28, H, 10.34, N, 6.47. IR (neat, cm^{-1}): 3058 (w), 3021 (w), 2959 (s), 2868 (m), 1662 (s), 1590 (w), 1445 (s), 1363 (m), 1356

(m), 1328 (w), 1279 (w), 1251 (w), 1172 (m), 1109 (w), 1075 (w). **Enamine/Imine Tautomer:**

Only NMR signals that are distinctive for this isomer are listed. ^1H NMR (500 MHz, CDCl_3) δ 13.5 (s, 1H, NH), 3.2 ($J = 7$, sept., 4H, $i\text{Pr}$ -methine), 2.1 (s, 3H, α -methyl), 1.9 (s, β -methyl), 1.3 ($J = 7$, d, $i\text{Pr}$ -methyl), 1.2 ($J = 7$, d, $i\text{Pr}$ -methyl) ppm. ^{13}C NMR (500 MHz, CDCl_3) δ 161.1 (β -C), 142.38 (*i*-C), 141.3 (*o*-C), 124.9 (*p*-Ar), 123.2 (*m*-C), 95.1 (α -C), 28.3 ($i\text{Pr}$ -CH), 24.3 ($i\text{Pr}$ -methyl), 23.6 ($i\text{Pr}$ -methyl), 18.9 (β -methyl), 16.0 (α -methyl) ppm. MS (EI^+) *m/z* (relative intensity): 433 (100%), 434 (32%), 435 (6%).

$\text{K}^{\text{Me}}\text{L}^{\text{Me}} \cdot \text{Et}_2\text{O}$. Benzylpotassium³ (5.24 g, 40.2 mmol) was added to a cooled solution (-78 °C) of $\text{H}^{\text{Me}}\text{L}^{\text{Me}}$ (15.9 g, 36.7 mmol) in Et_2O (60 mL). The mixture was allowed to warm to room temperature over 3 hours. The reaction mixture was filtered through Celite and dried under vacuum. The yellow solids were dissolved in Et_2O (~40 mL) and cooled to -35 °C to yield crystals (12.3 g, 26.1 mmol, 71%). ^1H NMR (500 MHz, C_6D_6) δ 7.1 (d, $J = 8$ Hz, 4H, *m*-aryl), 7.0 (t, $J = 8$ Hz, 2H, *p*-aryl), 3.3 (sept., $J = 7$ Hz, 4H, $i\text{Pr}$ -methine), 3.2 (q, $J = 7$ Hz, 4H, Et_2O), 2.3 (s, 3H, α -methyl), 2.0 (s, 6H, β -methyl), 1.2 (d, $J = 7$ Hz, 12H, $i\text{Pr}$ -methyl), 1.1 (t, $J = 7$ Hz, 6H, Et_2O) 1.0 (d, $J = 7$ Hz, 12H, $i\text{Pr}$ -methyl) ppm. ^{13}C NMR (500 MHz, C_6D_6) δ 159.9 (β -C), 151.0 (*i*-C), 139.5 (*o*-C), 123.8 (*m*-C), 120.5 (*p*-C), 91.4 (α -C), 65.9 (Et_2O), 27.6 ($i\text{Pr}$ -methine), 24.3 ($i\text{Pr}$ -methyl), 24.2 ($i\text{Pr}$ -methyl), 22.4 (β -methyl), 19.0 (α -methyl), 15.5 (Et_2O) ppm. Anal. Calcd for $\text{C}_{34}\text{H}_{53}\text{KN}_2\text{O}$: C, 74.94, H, 9.80, N, 5.14. Found: C, 75.16, H, 9.80, N, 5.09. IR (KBr, cm^{-1}): 3054 (w), 2959 (s), 2919 (m), 2867 (m), 1559 (m), 1456 (s), 1383 (s), 1307 (s), 1226 (m), 1181 (m), 1097 (m), 1058 (w), 981 (m), 935 (w), 818 (w), 774 (m), 706(w).

[^{Me}L^{Me}FeCl]₂. K^{Me}L^{Me} · Et₂O (1.3 g, 2.4 mmol) was mixed with FeCl₂(THF)_{1.5} (0.56 g, 2.4 mmol) in toluene (150 mL) at 100 °C overnight. The dark red solution was filtered through a fritted funnel. The filtrate was collected, concentrated and cooled to -35 °C to yield red crystals (0.74 g, 0.71 mmol, 59%). ¹H NMR (500 MHz, C₆D₆) δ 188 (6H, α-methyl), 11.1 (24H, ⁱPr-methyl), 8.9 (8H), -25.9 (8H), -34.2 (12H, β-methyl), -37.4 (24H, ⁱPr-methyl), -54.1 (4H, *p*-aryl) ppm. 8H resonances could be the ⁱPr-methine protons or the *m*-aryl protons. Anal. Calcd for C₆₀H₈₆Cl₂Fe₂N₄: C, 68.90, H, 8.29, N, 5.36. Found: C, 68.87, H, 8.57, N, 5.21. UV-Vis (mM⁻¹ cm⁻¹): 342(32), 539(0.3). μ_{eff} (Evans, THF-*d*₈): 5.3(4) μ_B. IR (KBr, cm⁻¹): 3057 (w), 2965 (s), 2926 (m), 2867 (m), 1521 (s), 1472 (s), 1462 (s), 1437 (s), 1419 (s), 1383 (m), 1364 (m), 1332 (s), 1312 (s), 1254 (m), 1239 (m), 1205 (w), 1180 (m), 1161 (w), 1132 (w), 1100 (w), 1076 (w), 1056 (w), 1039 (w), 989 (m), 935 (w), 864 (w), 802 (w), 780 (m), 728 (w).

^{Me}L^{Me}FeⁱBu. An analogous synthesis to L^{Me}FeⁱBu⁷ was used substituting K^{Me}L^{Me} for KL^{Me}. Additionally, 10 drops of 1,4 dioxane was added to the pentane crude reaction mixture before filtering. The reaction mixture was filtered twice through Celite (Yield 63%). ¹H NMR (500 MHz, C₆D₆) δ 193 (3H, α-methyl), 106 (6H, ⁱBu-methyl), 44.6 (6H, β-methyl), -10.7 (4H), -15.3 (12H, ⁱPr-methyl), -90.6 (2H, *p*-aryl), -110 (12H, ⁱPr-methyl), -137 (4H) ppm. 4H resonances could be the ⁱPr-methine protons or the *m*-aryl protons. The methylene group is close to the paramagnetic iron center so may be too broad to observe. The ¹H NMR spectrum closely resembled that of L^{Me}FeⁱBu.⁷ μ_{eff} (Evans, C₆D₆): 5.7(3) μ_B. UV-Vis (mM⁻¹ cm⁻¹): 300(13), 345(17), 398(10), 529(0.65). Anal. Calcd for C₃₄H₅₂FeN₂: C, 74.98, H, 9.62, N, 5.14. Found: C, 75.36, H, 9.90, N, 5.10. IR (KBr, cm⁻¹): 1529 (m), 1471 (w), 1457 (m), 1435 (m), 1424 (m), 1382 (w), 1367 (m), 1337 (s), 1314 (s),

1255 (w), 1240 (w), 1181 (w), 1159 (w), 1135 (w), 1099 (w), 1055 (w), 1041 (w), 994 (m), 935 (w), 866 (w), 809 (w), 794 (w), 784 (m), 757 (w), 734 (w), 704 (w), 668 (m), 643 (w), 618 (w), 562 (w).

Modified Synthesis and Characterization of $[L^{Me}Fe]_2(\mu-S)$ (1-H). $L^{Me}Fe^iBu$ (189.8 mg, 0.340 mmol) was mixed with Me_3PS (18.4 mg, 0.170 mmol) in toluene (20 mL) at 100 °C overnight. The volatile materials were evaporated. The solids were dissolved in pentane (20 mL) and filtered through Celite. The dark red filtrate was concentrated to 4 mL and cooled to -35 °C to yield crystals (108.9 mg, 0.111 mmol, 65%). **1-H** (58.0 mg, 59.2 μ mol) was dissolved in pentane (2 mL) and THF (0.5 mL) to form (1-H)(THF). 1H NMR (500 MHz, THF- d_8) δ 9.6 (8H), 1.6 (24H, i Pr-methyl), -2.3 (8H), -6.7 (4H, *p*-aryl), -7.4 (12H, β -methyl), -10.0 (24H, i Pr-methyl) ppm. A peak for the α -H was not seen, most likely due to broadening or overlap. 8H resonances could be the i Pr-methine protons or the *m*-aryl protons. This compound has been fully characterized in a previous publication,¹³ and the 1H NMR spectrum matches.

$[^{Me}L^{Me}Fe]_2(\mu-S)$ (1-Me). An analogous synthesis to (1-H) was used substituting $^{Me}L^{Me}Fe^iBu$ for $L^{Me}Fe^iBu$ (Yield 73%). 1H NMR (500 MHz, C_6D_6) δ 52.5 (6H, α -methyl), 14.9 (12H, β -methyl), 4.5 (8H), -0.9 (24H, i Pr-methyl), -12.8 (8H), -16.5 (4H, *p*-aryl), -19.8 (24H, i Pr-methyl) ppm. 1H NMR (500 MHz, THF- d_8) δ 47.8 (6H, α -methyl), 7.2 (8H), 1.9 (24H, i Pr-methyl), -4.6 (8H), -7.8 (12H, β -methyl), -10.0 (4H, *p*-aryl), -11.4 (24H, i Pr-methyl). 8H resonances could be the i Pr-methine protons or the *m*-aryl protons. The 1H NMR spectrum closely resembles the spectrum previously reported for $[L^{Me}Fe]_2(\mu-S)$ (1-H).¹³ μ_{eff} (Evans, THF- d_8): 5.1(5) μ_B . UV-Vis ($mM^{-1} cm^{-1}$): 308(29), 344(33), 391(28), 545(1.2). Anal. Calcd for $C_{60}H_{86}Fe_2N_4S$: C, 71.56, H, 8.61, N, 5.56.

Found: C, 71.85, H, 8.73, N, 5.23. IR (KBr, cm^{-1}): 3057 (w), 2958 (s), 2925 (m), 2865 (m), 1526 (m), 14612 (w), 1421 (w), 1383 (w), 1364 (w), 1337 (s), 1314 (s), 1253 (w), 1241 (w), 1181 (w), 1133 (w), 1101 (w), 1056 (w), 992 (m), 935 (w), 868 (w), 798 (w), 781 (m), 761 (m), 730 (w), 704 (w), 640 (w).

[K^{Me}L^{Me}Fe]₂(μ-S) (2-Me). **1-Me** (168 mg, 0.166 mmol) was added to a stirring solution of potassium graphite (49.4 mg, 0.366 mmol) in Et₂O (15 mL) causing an immediate color change to dark green. The mixture was stirred for 30 minutes, filtered through a plug of Celite and the solvent was evaporated under vacuum. The solids were dissolved in pentane (6 mL) and cooled to -35 °C to yield dark green crystals (111 mg, 0.10 mmol, 62%). ¹H NMR (500 MHz, C₆D₆) δ 28.4 (6H, α-methyl), 12.4 (8H), 4.5 (8H), 1.2 (24H, ⁱPr-methyl), -2.4 (24H, ⁱPr-methyl), -2.9 (4H, *p*-Aryl), -59.8 (12H, β-methyl) ppm. ¹H NMR (500 MHz, THF-*d*₈) δ 29.0 (6H, α-methyl), 12.7 (8H), 6.9 (4H, *p*-Aryl), 4.6 (8H), 1.2 (24H, ⁱPr-methyl), -2.8 (24H, ⁱPr-methyl), -62.6 (12H, β-methyl) ppm. 8H resonances could be the ⁱPr-methine protons or the *m*-aryl protons. μ_{eff} (Evans, C₆D₆): 2.6(3) μ_B. UV-Vis (mM⁻¹ cm⁻¹): 306(36), 375(17), 461(13), 681(sh, ~11), 753(14), 900(2.2). IR (KBr, cm^{-1}): 3050 (w), 2967 (s), 2926 (m), 2864 (m), 1574 (w), 1530 (w), 1462 (m), 1429 (m), 1405 (m), 1381 (w), 1354 (w), 1326 (vs), 1236 (m), 1190 (w), 1098 (m), 1058 (w) cm⁻¹. Anal. Calcd for C₆₀H₈₆Fe₂K₂N₄S: C, 66.40, H, 7.99, N, 5.16. Found: C, 66.70, H, 8.37, N, 4.96.

[KL^{Me}Fe]₂(μ-S) (2-H). An analogous procedure was used as for [K^{Me}L^{Me}Fe]₂(μ-S) (2-Me) substituting [L^{Me}Fe]₂(μ-S) (1-H) for **1-Me** (71% yield). ¹H NMR (500 MHz, C₆D₆) δ 12.1 (8H), 4.8 (8H), 1.3 (24H, ⁱPr-methyl), -1.5 (4H, *p*-Aryl), -2.5 (24H, ⁱPr-methyl), -16.4 (2H, α-H), -64.3 (12H, β-Me). 4H resonances could be the ⁱPr-methine protons or the *m*-aryl protons. μ_{eff} (Evans, C₆D₆):

3.0(2) μ_B . UV-Vis ($\text{mM}^{-1} \text{cm}^{-1}$): 300(43), 368(sh, 20), 450(16), 670(sh, 11), 768(14), 920(2.4). IR (KBr, cm^{-1}): 3055 (w), 2957 (s), 2921 (m), 2862 (m), 1566 (w), 1513 (m), 1459 (m), 1427 (s), 1388 (s), 1321 (s), 1257 (m), 1174 (w), 1100 (w), 1003 (w). Anal. Calcd for $\text{C}_{58}\text{H}_{82}\text{Fe}_2\text{K}_2\text{N}_4\text{S}$: C, 65.89, H, 7.82, N, 5.30. Found: C, 66.03, H, 8.00, N, 5.22.

[Na^{Me}L^{Me}Fe]₂(μ-S) (3-Me). Sodium metal (46.5 mg, 2.0 mmol) was weighed out in a vial making sure to expose a high surface area. **1-Me** (208 mg, 0.21 mmol) was dissolved in THF (20 mL) and pipetted onto the Na⁰ and stirred for 1.5 hours. The solution was decanted from the sodium, pumped down to solids and redissolved in pentane (10 mL). The solution was filtered through Celite, discarding the first few drops, concentrated and cooled to -35 °C to give dark green crystals (122 mg, 0.12 mmol, 56%). Characterization by of the dark green product by ¹H NMR spectroscopy showed a very similar peak pattern as **2-Me**. ¹H NMR (500 MHz, C_6D_6) δ 30.3 (6H, α-methyl), 13.5 (8H), 3.5 (8H), 1.4 (24H, ⁱPr-methyl), -2.6 (24H, ⁱPr-methyl), -6.3 (4H, *p*-Aryl), -57.7 (12H, β-methyl) ppm. ¹H NMR (500 MHz, THF-d₈) δ 30.2 (6H, α-methyl), 13.8 (8H), 6.9 (8H), 0.9 (24H, ⁱPr-methyl), -2.9 (24H, ⁱPr-methyl), -6.0 (4H, *p*-Aryl), -58.5 (12H, β-methyl) ppm. 8H resonances could be the ⁱPr-methine protons or the *m*-aryl protons. μ_{eff} (Evans, C_6D_6): 2.7(2) μ_B . UV-Vis ($\text{mM}^{-1} \text{cm}^{-1}$): 301(28), 467(12), 658(10), 705(10), 889(1.5). IR (KBr, cm^{-1}): 3057 (w), 2958 (s), 2926 (m), 2907 (m), 2865 (m), 1575 (w), 1526 (w), 1462 (m), 1431 (m), 1409 (m), 1382 (w), 1344 (s), 1320 (s), 1261 (w), 1237 (m), 1192 (w), 1100 (m) cm^{-1} . Calcd with 1 pentane molecule $\text{C}_{65}\text{H}_{98}\text{Fe}_2\text{N}_4\text{Na}_2\text{S}$: C, 69.38, H, 8.78, N, 4.98. Found: C, 69.48, H, 8.66, N, 4.88.

Cation Exchange Reactions in C₆D₆ and Et₂O

2-Me (5 mg, 5 µmol) was dissolved in 0.8 mL C₆D₆ or Et₂O, and sealed in a J. Young NMR tube with a Cp₂Co capillary standard in C₆D₆. **3-Me** was quantified by ¹H NMR spectroscopy. **3-Me** (5 mg, 5 µmol) in 0.4 mL C₆D₆ or Et₂O was added and mixed on a rotator. The reaction was monitored by ¹H NMR spectroscopy for 48 hours. Not all peaks for **4-Me** were distinguishable because of overlap. The ¹H NMR spectra can be seen below (Figure S-2).

Addition of external K⁺ and Na⁺ sources

2-Me (5 mg, 5 µmol) was dissolved in 0.8 mL Et₂O and sealed in a J. Young NMR tube with a Cp₂Co capillary standard in C₆D₆. An ¹H NMR spectrum was taken to check for purity. Na[BAr^F₄] (10 mg, 10 µmol) was dissolved and added to **2-Me**. Another ¹H NMR spectrum was obtained followed by addition of subsequent equivalents of Na[BAr^F₄]. Growth of peaks assigned to **4-Me** was seen as well as peaks corresponding to **3-Me** once two equivalents of Na[BAr^F₄] were added. The fraction of each species could not be determined quantitatively because of overlap and low resolution (¹H NMR spectra were taken in Et₂O for solubility reasons).

An analogous procedure was used for **3-Me** where KOTf was used as the K⁺ source.

The ¹H NMR spectra can be seen below (Figure S-3 and Figure S-4).

Control experiments

2-Me (5 mg, 5 µmol) and KOTf (50 mM solution in Et₂O, 0.1 mL, 5 µmol) were mixed in Et₂O (0.9 mL) and no growth of new peaks was seen over multiple hours.

3-Me (5 mg, 5 μmol) and $\text{Na[BAr}^{\text{F}}_4]$ (5 mg, 5 μmol) were mixed in Et_2O (1.2 mL) and no growth of new peaks was seen over multiple hours.

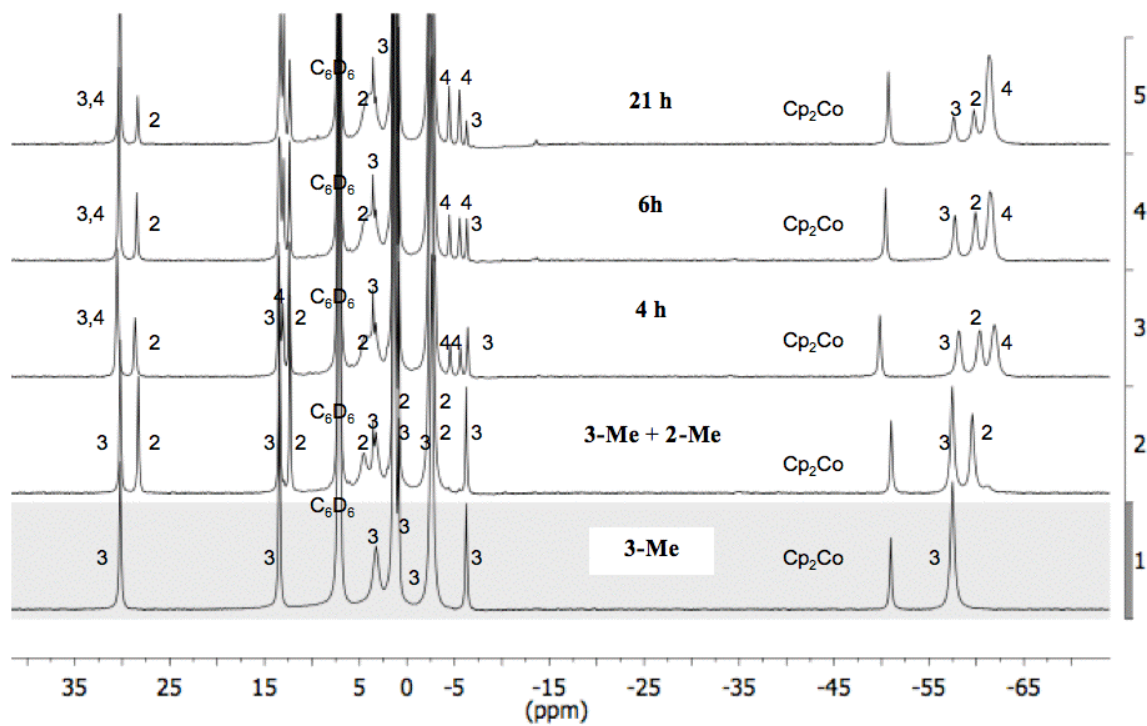


Figure S-2: Cation exchange between **2-Me** and **3-Me**. Compounds were dissolved in C_6D_6 and reaction was monitored by ^1H NMR spectroscopy with a Cp_2Co capillary standard (-51 ppm). The peaks for each compound are labeled by their compound number from the text. Peaks corresponding to **4-Me** lie at δ 30.2, 13.0, -4.4, -5.5, -61.2 ppm.

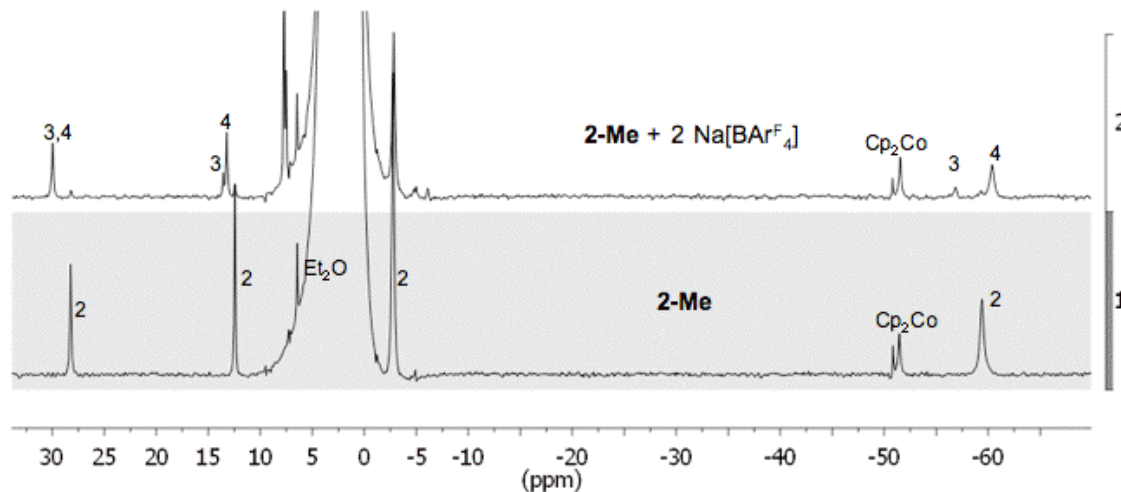


Figure S-3: Cation exchange by addition of 2 equiv of Na[BAr^F₄] to **2-Me** in Et₂O. The reaction was monitored by by ¹H NMR spectroscopy with a Cp₂Co capillary standard (-51 ppm).

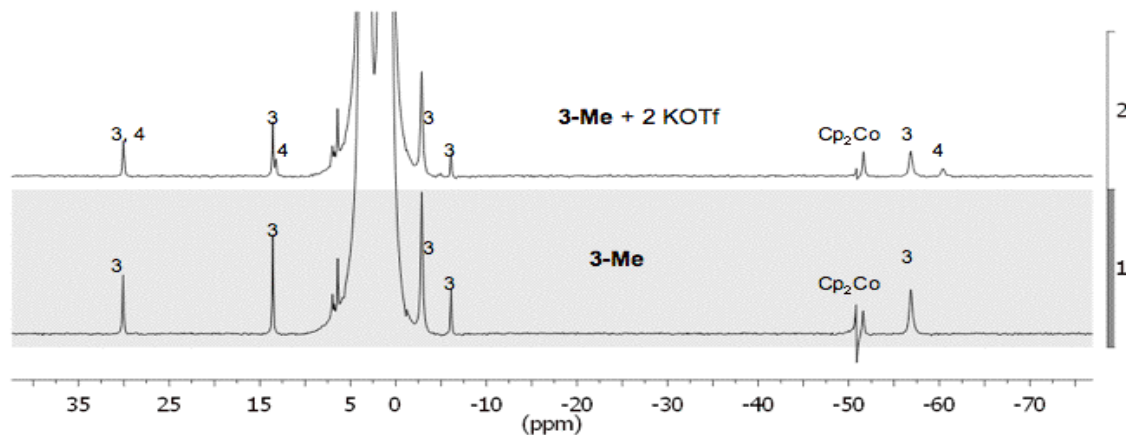


Figure S-4: Cation exchange by addition of 2 equiv of KOTf to **3-Me** in Et₂O. The reaction was monitored by by ¹H NMR spectroscopy with a Cp₂Co capillary standard (-51 ppm).

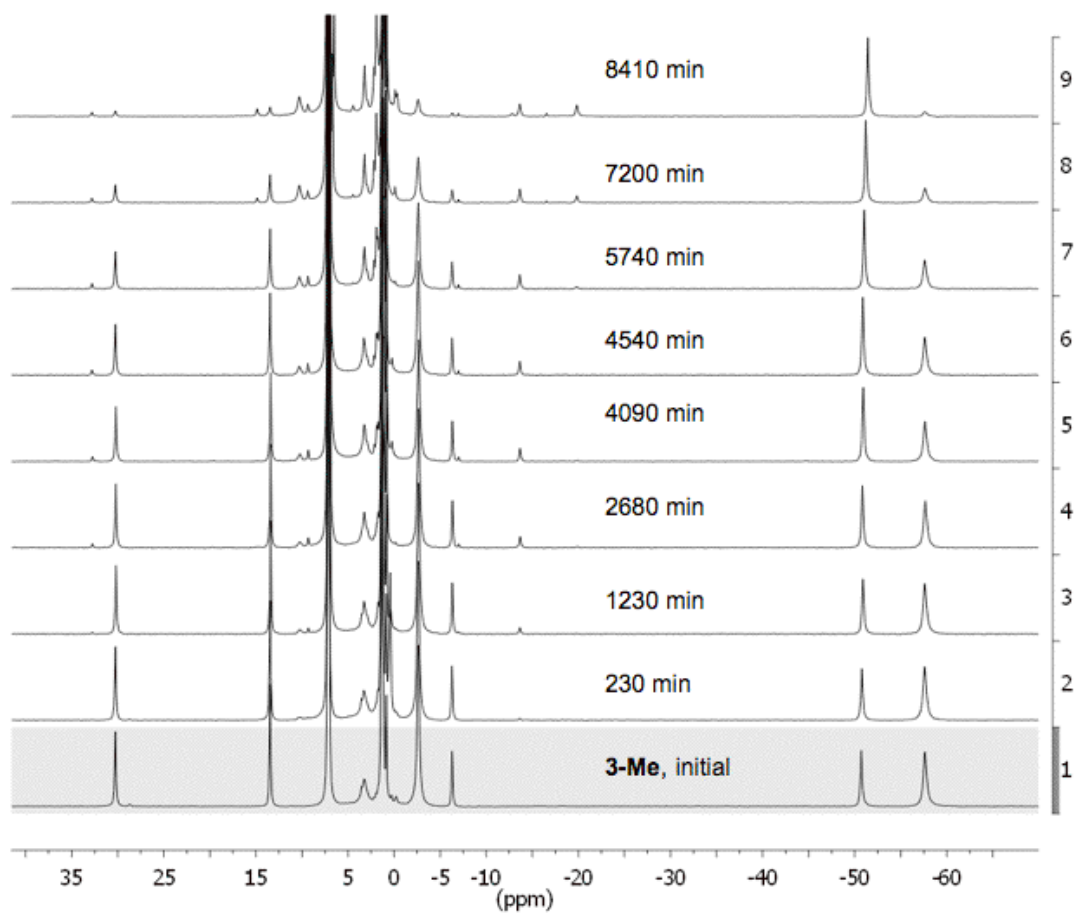


Figure S-5: Decomposition of **3-Me** in C₆D₆ at 60 °C. The reaction was monitored by by ¹H NMR spectroscopy with a Cp₂Co capillary standard (-51 ppm).

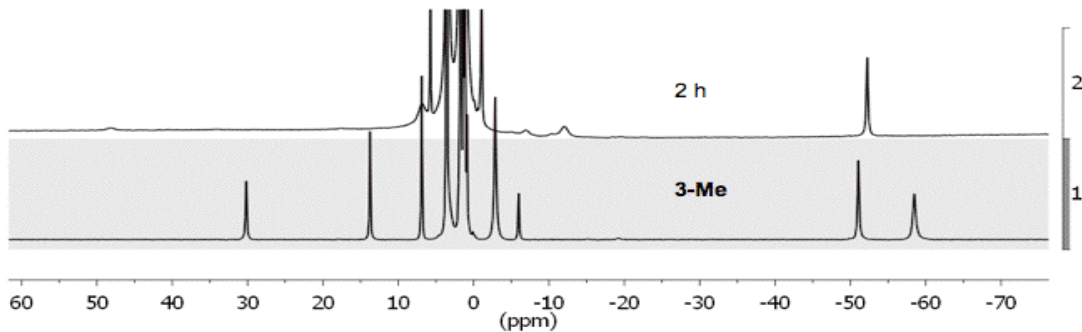


Figure S-6: Decomposition of **3-Me** in $\text{THF}-d_8$ at $60\text{ }^\circ\text{C}$. The reaction was monitored by ^1H NMR spectroscopy with a Cp_2Co capillary standard (-51 ppm).

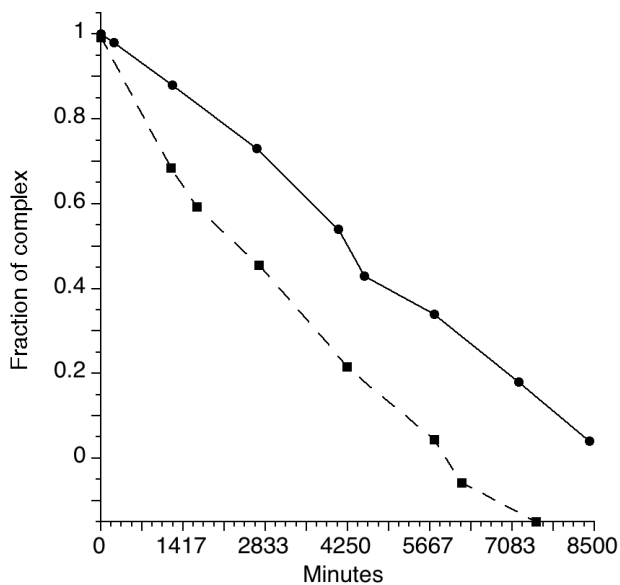


Figure S-7: Decomposition of $[\text{M}_\text{A}\text{LF}_\text{e}]_2(\mu\text{-S})$ compounds at $60\text{ }^\circ\text{C}$ in C_6D_6 . A solution of 2.9 mM $[\text{K}^{\text{Me}}\text{L}^{\text{Me}}\text{Fe}]_2(\mu\text{-S})$ (**2-Me**, dashed line, square markers) or 2.4 mM $[\text{Na}^{\text{Me}}\text{L}^{\text{Me}}\text{Fe}]_2(\mu\text{-S})$ (**3-Me**, solid line, circle markers) in C_6D_6 was monitored by ^1H NMR spectroscopy, and the integrations of the $\alpha\text{-Me}$ and $\beta\text{-Me}$ peaks were compared to that of an internal standard of $(\text{C}_5\text{H}_5)_2\text{Co}$ in C_6D_6 .

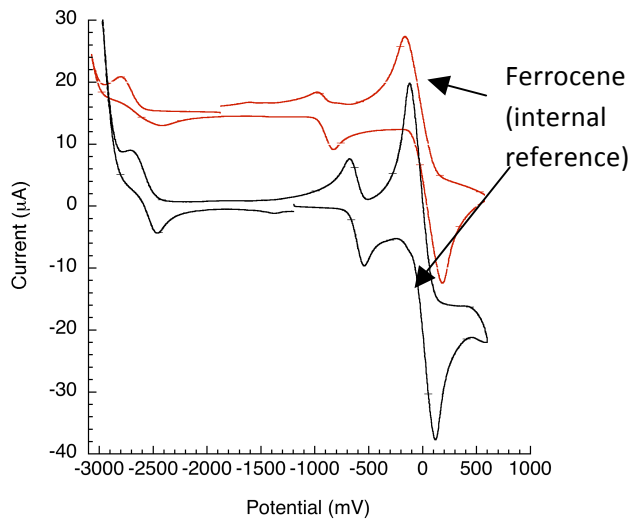


Figure S-8. Comparison of CV in diethyl ether and THF with 50 mM [NBu₄][BAr₄]^F. Black line: Cyclic voltammogram of 2 mM **1-Me** in Et₂O. The E_{1/2} values are -0.7 V for the oxidation wave and -2.7 V for the reduction wave, vs. a ferrocene reference. Notice that the sizes of these waves are similar, implying that the same number of electrons are passed. Red line: Cyclic voltammogram of 2 mM **1-Me** in THF. The E_{1/2} values are -0.9 V for the oxidation wave and -2.6 V for the reduction wave, vs. a ferrocene reference. Since THF binds to **1-Me** (data not shown), it is reasonable that both waves occur at more positive potentials (THF binding stabilizes the more oxidized form).

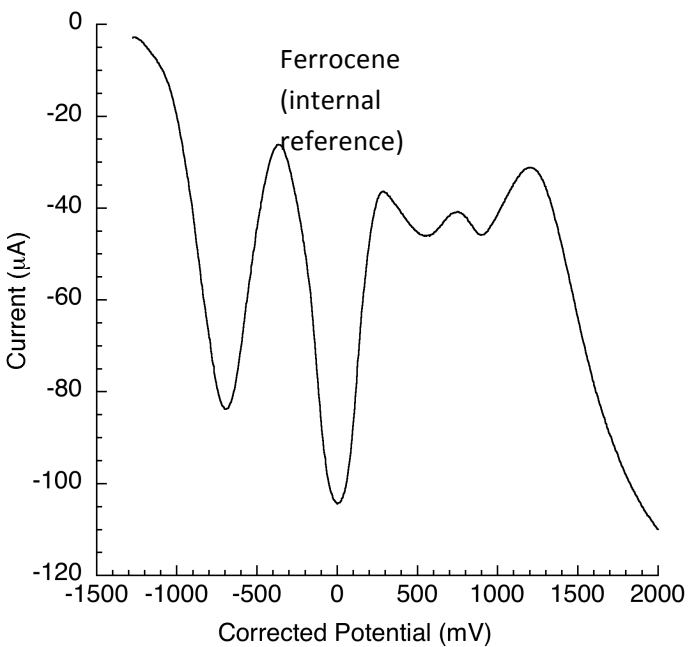


Figure S-9. Differential pulse voltammogram of a sample of **1-Me** (3.8 mM), ferrocene (3.8 mM) with 50 mM $[\text{NBu}_4]^+ \text{[BAr}^{\text{F}}_4]$ in Et_2O . The voltammogram is shown in the oxidizing direction. The oxidation wave for the diiron sulfide complex is observed at -0.7 V, and ferrocene at 0.0 V. The similar heights of the peaks show that both redox events involve the same number of electrons, and therefore the oxidation of **1-Me** is a one-electron event like ferrocene oxidation. Because the oxidation and reduction waves in the cyclic voltammogram of **1-Me** (Figure S-8) are the same size, it is most likely that the reduction of **1-Me** is also a one-electron event. Therefore, the **1-Me** reduction wave in the CV *does not* correspond to formation of a diiron(I) complex (**2-Me** or **3-Me**). We have been unable to isolate any mixed-valence iron(I)iron(II) complexes, despite numerous attempts with different strategies. Therefore, the nature of the presumed intermediates during formation of **2-Me** and **3-Me** remains unknown.

Magnetic susceptibility. Magnetic susceptibility data were measured with powder samples in the temperature range 2 - 300 K using a SQUID susceptometer (MPMS-7, Quantum Design) with a field of 1.0 T. The experimental data were corrected for underlying diamagnetism by use of tabulated Pascal's constants,^{15, 16} as well as for temperature-independent paramagnetism. The susceptibility and magnetization data were simulated with our own package juIX for exchange coupled systems.¹⁷ The simulations are based on the spin-Hamilton operator for two identical Fe(I) high-spin ions with spins $S_1 = S_2 = 3/2$:

$$\hat{H} = -2J \hat{\vec{S}}_1 \cdot \hat{\vec{S}}_2 + g\beta(\hat{\vec{S}}_1 + \hat{\vec{S}}_2) \cdot \vec{B} \quad (1)$$

where J is the exchange coupling constants and g represents the average electronic g values for both iron sites. Zero-field splitting was neglected in the simulation of the magnetic data of (2) because the ground state of the coupled spin system is a singlet ($S = 0$) and the measurements are not sensitive to the corresponding weak splitting of the excited states, the first of which ($S = 1$) is at an energy of 246 cm^{-1} (the spin ladder has states with spin S at energies $E(S) = -J S(S+1)$). Diagonalization of the Hamiltonian was performed with the routine ZHEEV from the LAPACK Library¹⁸ and the magnetic moments were obtained from the eigenfunctions using the Hellman-Feyman theorem $dE_i/dB = \langle \psi_i | dH/dB | \psi_i \rangle$. The powder summations were done by using a 16-point Lebedev grid.^{19,20}

Mössbauer Spectroscopy. Mössbauer data were recorded on a spectrometer with alternating constant acceleration. The minimum experimental line width was 0.24 mm s^{-1} (full width at half-height). The sample temperature was maintained constant either in an Oxford Instruments Variox or an Oxford Instruments Mössbauer-Spectromag cryostat. The latter is a split-pair super-conducting magnet system for applied fields up to 8 T where the temperature of the sample can be varied in the range 1.5 K to 250 K. The field at the sample is perpendicular to the γ -beam. The $^{57}\text{Co}/\text{Rh}$ source (1.8 GBq) was positioned at room temperature inside the gap of the magnet system at a zero-field position. Isomer shifts are quoted relative to iron metal at 300 K. Magnetic Mössbauer spectra were simulated with the usual nuclear Hamiltonian.²¹

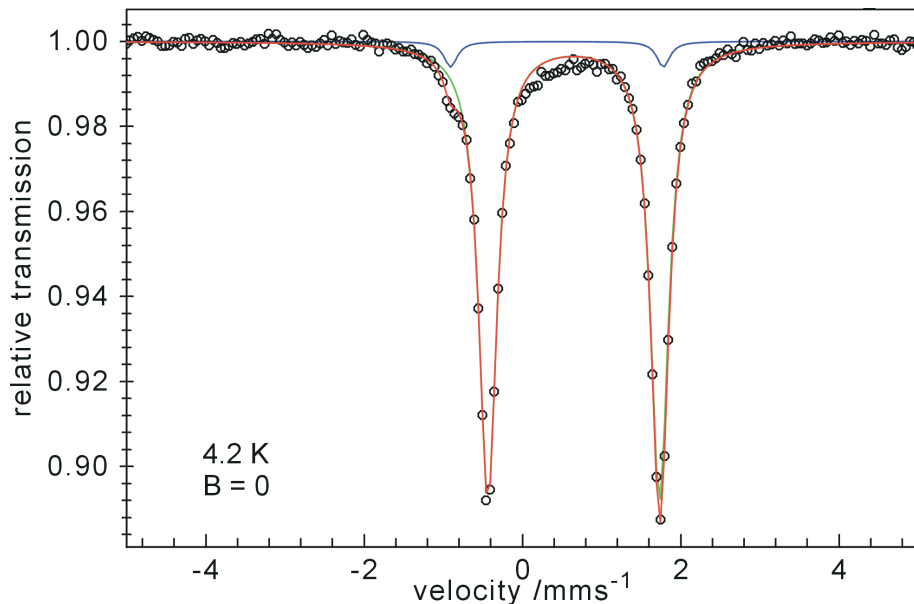


Figure S-10. Zero-field Mössbauer spectrum of solid **2-Me** recorded at 4.2 K. A second sample had to be used, since the first one, used for Figure 2a (top) had been decomposed after storage in liquid nitrogen. This sample was also used for the applied field measurement depicted in figure 2a (bottom). The Mössbauer parameters of the main component (96%) are $\delta = 0.67 \text{ mm s}^{-1}$, $\Delta E_Q = 2.17 \text{ mm s}^{-1}$, which is identical to the values observed at 80 K. The minor component (blue line, 4%) shows $\delta = 0.44 \text{ mm s}^{-1}$, $\Delta E_Q = 2.69 \text{ mm s}^{-1}$.

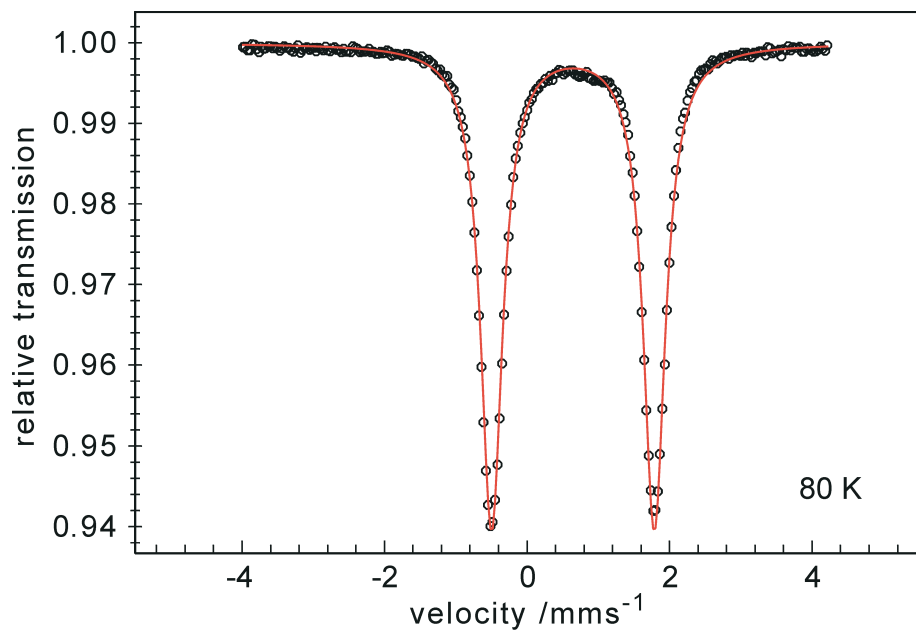


Figure S-11. Zero-field Mössbauer spectrum of solid **3-Me** recorded at 80 K. The Mössbauer parameters obtained from a fit with Lorentzian lines are $\delta = 0.64 \text{ mm s}^{-1}$, $\Delta E_Q = 2.28 \text{ mm s}^{-1}$.

References

- (1) Evans, D. F. *J. Chem. Soc.* **1959**, 2003-5.
- (2) Schubert, E. M. *J. Chem. Educ.* **1992**, 69, 62.
- (3) Bailey, P. J.; Coxall, R. A.; Dick, C. M.; Fabre, S.; Henderson, L. C.; Herber, C.; Liddle, S. T.; Lorono-Gonzalez, D.; Parkin, A.; Parsons, S. *Chem. Eur. J.* **2003**, 9, 4820-4828.
- (4) Stender, M.; Wright, R. J.; Eichler, B. E.; Prust, J.; Olmstead, M. M.; Roesky, H. W.; Power, P. P. *J. Chem. Soc., Dalton Trans.* **2001**, 3465-3469.
- (5) Feldman, J.; McLain, S. J.; Parthasarathy, A.; Marshall, W. J.; Calabrese, J. C.; Arthur, S. D. *Organometallics* **1997**, 16, 1514-1516.
- (6) Kern, R. J. *J. Inorg. Nucl. Chem.* **1962**, 24, 1105-9.
- (7) Vela, J.; Vaddadi, S.; Cundari, T. R.; Smith, J. M.; Gregory, E. A.; Lachicotte, R. J.; Flaschenriem, C. J.; Holland, P. L. *Organometallics* **2004**, 23, 5226-5239.
- (8) Jones, W. D.; Selmezy, A. D. *Organometallics* **1992**, 11, 889-93.
- (9) Yakelis, N. A.; Bergman, R. G. *Organometallics* **2005**, 24, 3579-3581.
- (10) Le Bras, J.; Jiao, H.; Meyer, W. E.; Hampel, F.; Gladysz, J. A. *J. Organomet. Chem.* **2000**, 616, 54-66.
- (11) Budzelaar, P. H. M.; Moonen, N. N. P.; de Gelder, R.; Smits, J. M. M.; Gall, A. W. *Eur. J. Inorg. Chem.* **2000**, 753-769.
- (12) Eckert, N. A.; Smith, J. M.; Lachicotte, R. J.; Holland, P. L. *Inorg. Chem.* **2004**, 43, 3306-3321.
- (13) Vela, J.; Stoian, S.; Flaschenriem, C. J.; Münck, E.; Holland, P. L. *J. Am. Chem. Soc.* **2004**, 126, 4522-4523.
- (14) Holland, P. L. *Acc. Chem. Res.* **2008**, 41, 905-914.
- (15) O'Connor, C. J. *Prog. Inorg. Chem.* **1982**, 29, 203-83.
- (16) Weast, R. C.; Astle, M.J. *CRC Handbook of Chemistry and Physics*. CRC Press Inc.: Boca Raton, Florida, 1979.
- (17) Available from E.B.: http://ewww.mpi-muelheim.mpg.de/back/logins/bill/julX_en.php.
- (18) The routines are available at <http://www.netlib.org/lapack/>.
- (19) Lebedev, V. I.; Laikov, D.N. *Doklady Math.* **1999**, 59, 477.
- (20) A Fortran code to generate Lebedev grids up to order L = 121 is available at <http://server.ccl.net/cca/software/SOURCES/>.
- (21) Trautwein, A. X.; Bill, E.; Bominaar, E. L.; Winkler, H., *Structure and Bonding* **1991**, 78, 1-95.

Computations. The electronic structure of **2-Me** has been calculated using density functional theory (DFT) as described previously for the related iron(I) hydride compounds¹ using the ORCA program.² The B3LYP³ and TPSSh⁴ functionals with various basis sets⁵⁻⁷ have been examined, and the effects of truncating the nacnac ligand and modeling dissolution in water using the conductor-like screening model (COSMO)⁸ have also been explored. All calculations used an empirical van der Waals correction to the DFT energy.⁹ To model the antiferromagnetic coupling, we performed our calculations on **2-Me** using Broken Symmetry DFT.^{10,11} We gauged the accuracy of our calculations by comparing the experimental Mössbauer parameters and antiferromagnetic exchange coupling constant (J) with the calculated values.^{11,12}

As with the iron(I) hydride complexes,¹ employing the TPSSh functional with the TZVP⁵ basis set at the iron using the atomic coordinates from the X-ray crystal structure (without geometry optimization) provided results that agreed with the experimentally determined values (Table S1).¹³ The agreement in the isomer shift is reasonable compared to the standard deviation (0.10 mm/s) of the isomer shifts in the "training set" used for the empirical determination of the calculated isomer shift from the calculated electron density at the iron atom.¹²

Table 1. Calculated (TPSSh/TZVP)⁴ and experimental isomer shift (δ), quadrupole splitting (ΔE_q), and antiferromagnetic exchange coupling constant (J)^{11a,b} for complex **2-Me**. Calculated values are from a single-point calculation on an all-atom model at the crystal-structure geometry.

	δ (mm s ⁻¹)	ΔE_q (mm s ⁻¹)	J (cm ⁻¹)
exp.	0.67	-2.17	-123
calc.	0.54	-1.85	-170

The electronic structure description of **2-Me** derived from our calculations reveals the presence of two antiferromagnetically-coupled high-spin Fe^I centers (Figure S12). A small degree of π -backbonding from the Fe^I centers to the diketiminate LUMOs is observed, but the amount of spin density on the diketiminate ligands is too small to indicate "redox non-innocence" (Figure S13).

Figure S12. (a) Simplified MO interaction diagram depicting the mechanism of antiferromagnetic exchange coupling between the two iron(I) centers. A filled and an unfilled orbital mix via configuration interaction, which is modeled here using broken symmetry DFT. Two of these interactions are present, using orbitals whose orientation differs by 90°. (b) Calculated MOs corresponding to the bonding (bottom) and antibonding (top) orbitals described in (a); the non-bonding orbitals are shown in the manuscript (top of Figure 3).

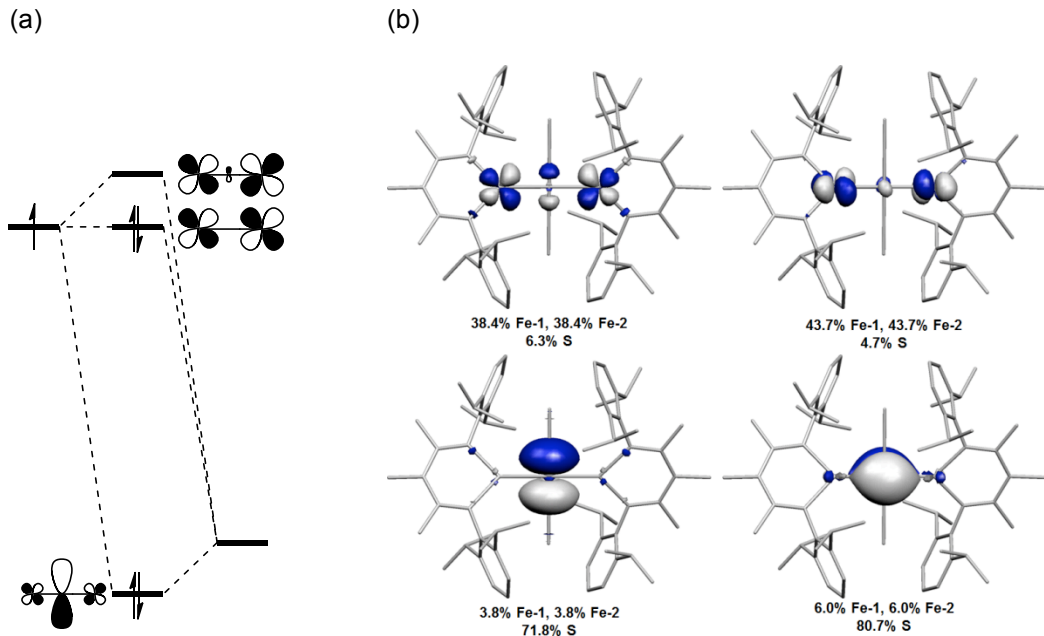
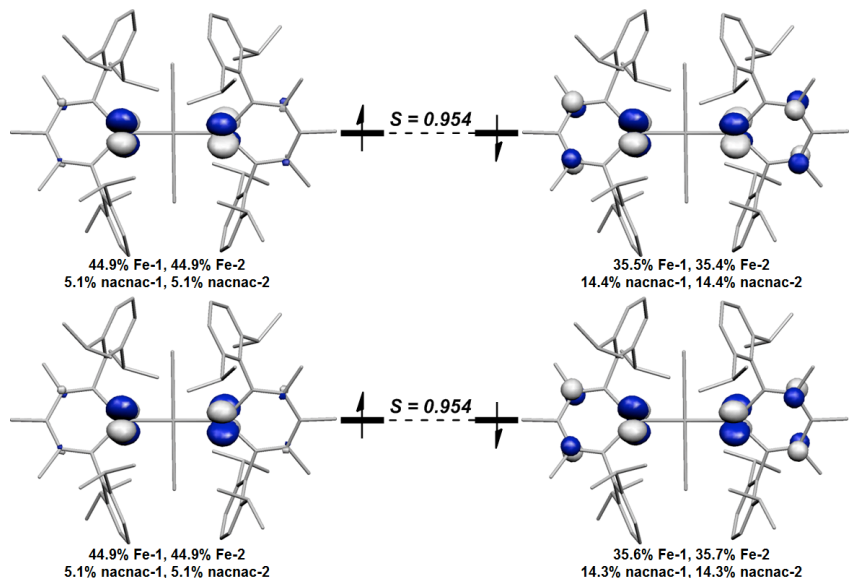


Figure S13. (a) Unrestricted corresponding orbital (UCO) picture of the HOMO–1 (bottom) and HOMO (top) of high-spin ($S_{\text{tot}} = 3$) **2-Me** (two ferromagnetically coupled high-spin Fe(I) ions). These orbitals are the only doubly-occupied MOs that have a spatial overlap between the alpha- and beta-spin components of less than 0.992 in the $S_{\text{tot}} = 3$ solution. The SOMOs of this calculation (b) are largely metal centered. This high-spin calculation has very low spin contamination (1.9%) and the doubly-occupied orbitals are qualitatively identical to those in the BS(3,3) ($S_{\text{tot}} = 0$) calculation, revealing that antiferromagnetic coupling between the two high-spin Fe(I) centers satisfactorily accounts for the spin contamination in the BS(3,3) calculation, providing further justification (beyond our calculated Mössbauer parameters and J value) for our use of broken-symmetry calculations in the present case. This calculation also shows that a slight amount of beta spin lies on the diketiminate ligand, but the overlaps between alpha and beta spins in the HOMO–1 and HOMO are too high to indicate "redox non-innocence."

(a)



(b)

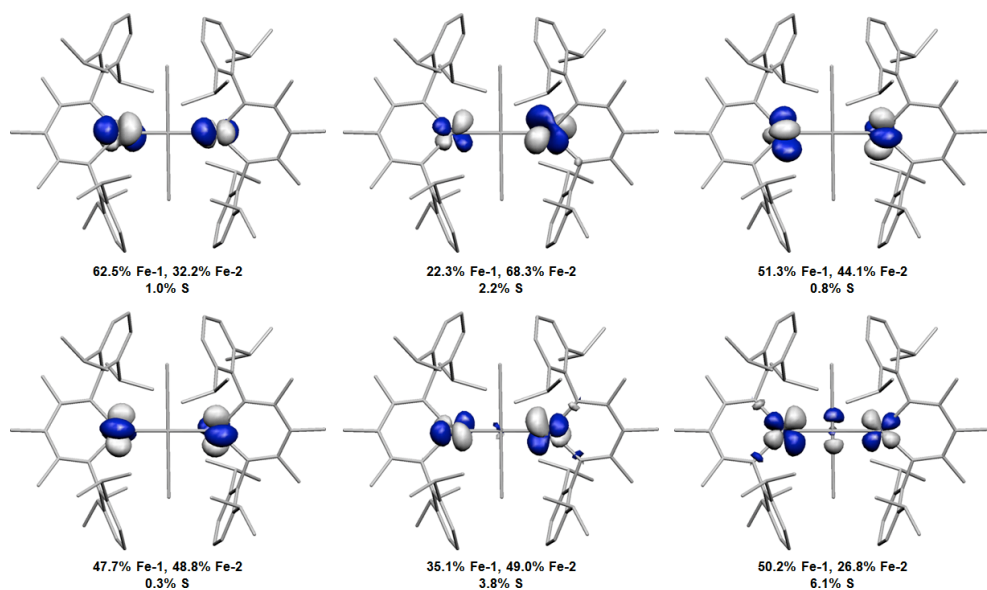


Table S1. Calculated Mössbauer parameters and antiferromagnetic exchange coupling constants (J) from single-point calculations on the crystal structure geometry of **2-Me** using various functionals and basis sets at the iron center. Calculations were performed using the broken-symmetry method BS(3,3), $S_{\text{total}} = 0$. Calculations using BS(5,5) – corresponding to two high-spin iron(II) ions with antiferromagnetically coupled ligand radicals – converged to the same solution as the BS(3,3) calculation. Experimental values: $\delta = 0.67 \text{ mm s}^{-1}$, $\Delta E_Q = -2.17 \text{ mm s}^{-1}$, $J = -123 \text{ cm}^{-1}$. The calculated values of ΔE_Q and δ for each iron center are identical.

functional	basis set at Fe	$\delta (\text{mm s}^{-1})$	$\Delta E_Q (\text{mm s}^{-1})$	$J (\text{cm}^{-1})$
B3LYP	TZVP	0.52	-1.78	-144
	CP(PPP)	0.50	-1.97	-143
TPSSh	TZVP	0.54	-1.85	-170
	CP(PPP)	0.41	-2.05	-168

Table S2. Calculated Mössbauer parameters from geometry-optimized calculations starting from the crystal-structure geometry of **2-Me** using various functionals and basis sets at the iron center. When the basis set CP(PPP) was used at iron, these calculations were run as single-point calculations on the corresponding TZVP-optimized geometry. Calculations were performed as described in the Experimental section of the manuscript (BS(3,3), $S_{\text{total}} = 0$). Experimental values: $\delta = 0.67 \text{ mm s}^{-1}$, $\Delta E_Q = -2.17 \text{ mm s}^{-1}$, $J = -123 \text{ cm}^{-1}$.

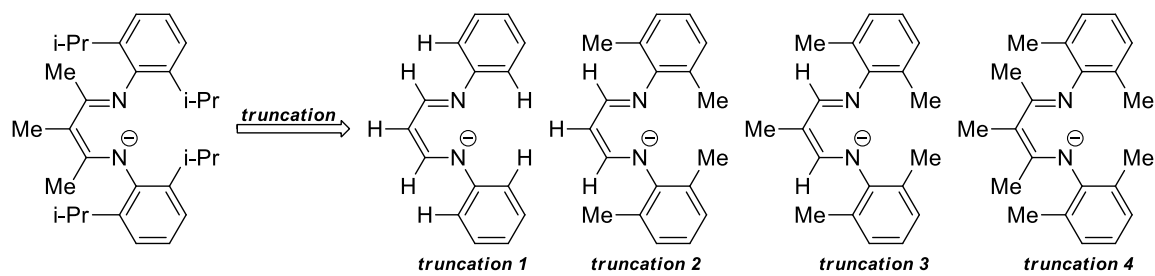
functional	basis set at Fe	$\delta (\text{mm s}^{-1})$	$\Delta E_Q (\text{mm s}^{-1})$	$J (\text{cm}^{-1})$
B3LYP	TZVP	0.63, 0.63	-1.56, -1.56	-31
	CP(PPP)	0.60, 0.60	-1.67, -1.67	-31
TPSSh	TZVP	0.60, 0.60	-1.74, -1.68	-96
	CP(PPP)	0.46, 0.45	-1.87, -1.80	-100
TPSS	TZVP	0.51, 0.51	-1.67, -1.67	-172
	CP(PPP)	0.51, 0.51	-1.85, -1.85	-173

Table S3. Calculated Mössbauer parameters from single-point calculations on the geometry from a TPSS geometry optimization starting from the crystal structure geometry of **2-Me** using various functionals and basis sets at the iron center. This set of calculations mimics an approach described previously (Römelt, M.; Ye, S.; Neese, F. *Inorg. Chem.* **2009**, *48*, 784). Calculations were performed as described in the Experimental section of the manuscript (BS(3,3), $S_{\text{total}} = 0$). Experimental values: $\delta = 0.67 \text{ mm s}^{-1}$, $\Delta E_Q = -2.17 \text{ mm s}^{-1}$, $J = -122 \text{ cm}^{-1}$. The calculated values of ΔE_Q and δ for each iron center are identical. Although the TPSSh/TZVP combination gives good agreement with experiment, the TPSS-optimized geometry has bonds to iron that are $\sim 0.04 \text{ \AA}$ longer than in the crystal-structure geometry, and we have therefore chosen to include the TPSSh/TZVP single-point calculation in the manuscript. Moreover, inspection of the orbitals and spin populations in the geometry-optimized model showed that they were similar to those derived from the X-ray coordinates, indicating that the conclusions in this paper are not very sensitive to these geometrical details.

functional	basis set at Fe	$\delta (\text{mm s}^{-1})$	$\Delta E_Q (\text{mm s}^{-1})$	$J (\text{cm}^{-1})$
B3LYP	TZVP	0.58	-1.76	-107
	CP(PPP)	0.55	-1.96	-108
TPSSh	TZVP	0.60	-1.80	-126
	CP(PPP)	0.46	-2.0	-127

Table S4. Calculated Mössbauer parameters of **2-Me** from single-point calculations using the TPSSh functional following nacnac truncation (see below) and TPSSh optimization of only the hydrogen atom positions. Calculations were run with and without the conductor-like screening model (COSMO) to mimic solvation in water. These results show that, using various levels of truncation, the inclusion of COSMO has an insignificant effect on the calculated Mössbauer parameters for this molecule, which is important because the full structure was too large to incorporate COSMO in the calculation and we had found COSMO to be important for calculating Mössbauer parameters of an *anionic* Fe(I)-hydride complex.¹

In all cases, the TZVP basis set was applied at the iron center. Calculations used broken symmetry (3,3), $S_{\text{total}} = 0$. Experimental values: $\delta = 0.67 \text{ mm s}^{-1}$, $\Delta E_Q = -2.17 \text{ mm s}^{-1}$, $J = -123 \text{ cm}^{-1}$. The calculated values of ΔE_Q and δ for each iron center are identical.



truncation	COSMO(water)	$\delta (\text{mm s}^{-1})$	$\Delta E_Q (\text{mm s}^{-1})$	$J (\text{cm}^{-1})$
1	yes	0.49	-1.76	-155
	no	0.51	-1.98	-155
2	yes	0.51	-1.91	-166
	no	0.51	-1.87	-166
3	yes	0.50	-1.91	-166
	no	0.51	-1.88	-167
4	yes	0.53	-1.75	-166
	no	0.53	-1.74	-167
none ^a	no	0.54	-1.88	

(a) Hydrogen atom positions of the full crystal-structure geometry were optimized. Implementation of COSMO failed with the full structure, presumably due to the size of this molecule.

Computational References

- (1) K. P. Chiang, C. C. Scarborough, M. Horitani, N. S. Lees, K. Ding, T. R. Dugan, W. W. Brennessel, E. Bill, B. M. Hoffman, P. L. Holland, *Angew. Chem. Int. Ed.* **2012**, *51*, in press.
- (2) Neese, F. *ORCA Ab Initio, Density Functional, and Semiempirical Electronic Structure Program Package, version 2.8*, Universität Bonn, Germany, 2011.
- (3) (a) Becke, A. D. *J. Chem. Phys.* **1993**, *98*, 5648. (b) Lee, C. T.; Yang, W. T.; Parr, R. G. *Phys. Rev. B* **1988**, *37*, 785.
- (4) Staroverov, V. N.; Scuseria, G. E.; Tao, J.; Perdew, J. P. *J. Chem. Phys.* **2003**, *119*, 12129.
- (5) Schäfer, A.; Huber, C.; Ahlrichs, R. *J. Chem. Phys.* **1994**, *100*, 5829.
- (6) (a) Becke, A. D. *J. Chem. Phys.* **1993**, *98*, 5648. (b) Lee, C.; Yang, W.; Parr, R. G. *Phys. Chem. B* **1988**, *37*, 785.
- (7) (a) Neese, F. *Inorg. Chim. Acta* **2002**, *337*, 181. (b) Sinnecker, S.; Slep, L. D.; Bill, E.; Neese, F. *Inorg. Chem.* **2005**, *44*, 2245.
- (8) Klamt, A.; Jonas, V.; Bürger, T.; Lohrenz, J. C. W. *J. Phys. Chem. A* **1998**, *102*, 5074.
- (9) (a) Grimme, S., *J. Comput. Chem.* **2004**, *25*, 1463-1476. (b) Grimme, S., *J. Comput. Chem.* **2006**, *27*, 1787-1799. (c) Grimme, S.; Antony, J.; Ehrlich, S.; Krieg, H., *J. Chem. Phys.* **2010**, *132*, 154104.
- (10) (a) Noddeman, L. *J. Chem. Phys.* **1981**, *74*, 5737. (b) Noddeman, L.; Case, D. A.; Aizman, A. *J. Am. Chem. Soc.* **1988**, *110*, 1001. (c) Noddeman, L.; Davidson, E. R. *Chem. Phys.*

1986, **109**, 131. (d) Noddleman, L.; Norman, J. G.; Osborne, J. H.; Aizman, A.; Case, D. A. *J. Am. Chem. Soc.* **1985**, **107**, 3418. (e) Noddleman, L.; Peng, C. Y.; Case, D. A.; Mouesca, J. M. *Coord. Chem. Rev.* **1995**, **144**, 199.

(11) (a) Yamaguchi, K.; Takahara, Y.; Fueno, T. In *Applied Quantum Chemistry*, Smith, V. H.; Ed.; Reidel: Dordrecht, 1986; p. 155. (b) Soda, T.; Kitagawa, Y.; Onishi, T.; Takano, Y.; Shigeta, Y.; Nagao, H.; Yoshioka, Y.; Yamaguchi, K. *Chem. Phys. Lett.* **2000**, **319**, 223-230. (c) Bencini, A.; Gatteschi, D. *J. Am. Chem. Soc.* **1980**, **108**, 5763.

(12) Römel, M.; Ye, S.; Neese, F. *Inorg. Chem.* **2009**, **48**, 784.

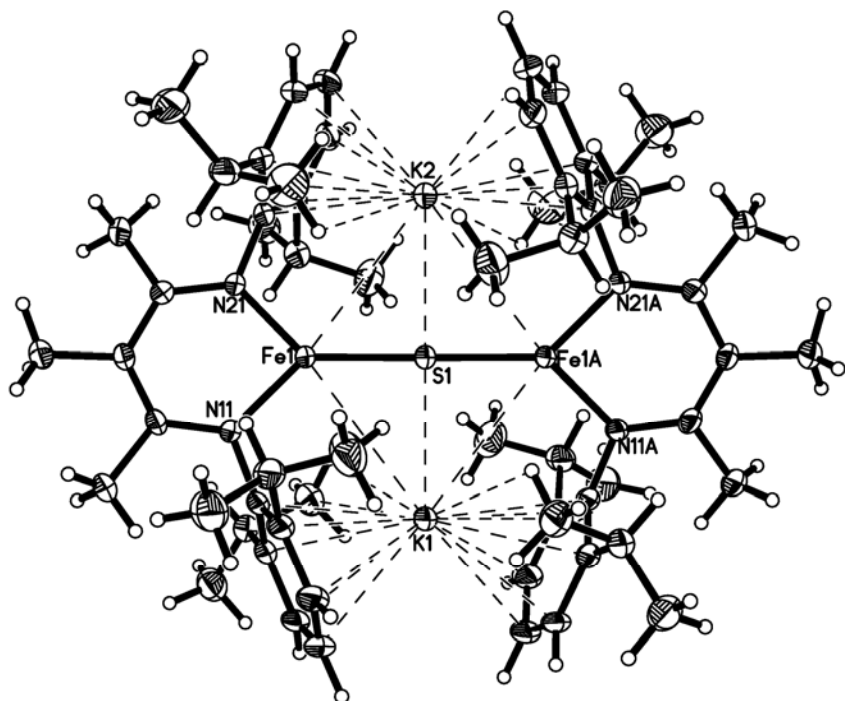
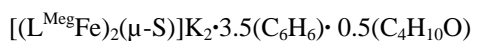
(13) The TPSSh functional was also found to provide the best calculated Mössbauer parameters for two dinitrosyl iron compounds: Ye, S.; Neese, F. *J. Am. Chem. Soc.* **2010**, **132**, 3646.

REFERENCE NUMBER: holmc10

CRYSTAL STRUCTURE REPORT



Or



Report prepared for:

Dr. Patrick Holland

Meghan Clark

February 18, 2009

Meghan Clark

X-ray Crystallographic Facility

Department of Chemistry, University of Rochester

120 Trustee Road

Rochester, NY 14627

Data collection

A crystal ($0.36 \times 0.28 \times 0.14 \text{ mm}^3$) was placed onto the tip of a 0.1 mm diameter glass capillary tube or fiber and mounted on a Bruker SMART APEX II CCD Platform diffractometer for a data collection at $100.0(1) \text{ K}$.¹ A preliminary set of cell constants and an orientation matrix were calculated from reflections harvested from three orthogonal wedges of reciprocal space. The full data collection was carried out using MoK α radiation (graphite monochromator) with a frame time of 45 seconds and a detector distance of 4.05 cm. A randomly oriented region of reciprocal space was surveyed: four major sections of frames were collected with 0.50° steps in ω at four different ϕ settings and a detector position of -38° in 2θ . The intensity data were corrected for absorption.² Final cell constants were calculated from the xyz centroids of 3822 strong reflections from the actual data collection after integration.³ See Table 1 for additional crystal and refinement information.

Structure solution and refinement

The structure was solved using SIR97⁴ and refined using SHELXL-97.⁴ The space group *Pbcn* was determined based on systematic absences and intensity statistics. A direct-methods solution was calculated which provided most non-hydrogen atoms from the E-map. Full-matrix least squares / difference Fourier cycles were performed which located the remaining non-hydrogen atoms. All non-hydrogen atoms were refined with anisotropic displacement parameters. All hydrogen atoms were placed in ideal positions and refined as riding atoms with relative isotropic displacement parameters. Reflection contributions from highly disordered co-crystallized solvent were removed using program PLATON, function SQUEEZE,⁶ which determined there to be 693 electrons in 2168 \AA^3 . The solvent, which packed in channels parallel to the *c*-axis, could be identified as 3.5 benzene molecules and 0.5 diethyl ether molecules per di-iron molecule. Since the identity of the solvent was known, it was included in the molecular formula but not in the atom list. The final full matrix least squares refinement converged to $R1 = 0.0645$ ($F^2, I > 2\sigma(I)$) and $wR2 = 0.1921$ (F^2 , all data).

Structure description

The structure is the one suggested. The di-iron molecule lies on a crystallographic 2-fold axis, coincident with the sulfur and two potassium atoms. The angle between the N-Fe-N and Fe-K-S-K planes is $16.67(5)$ degrees.

Unless noted otherwise all structural diagrams containing thermal displacement ellipsoids are drawn at the 50 % probability level.

Data collection, structure solution, and structure refinement were conducted at the X-ray Crystallographic Facility, B51 Hutchison Hall, Department of Chemistry, University of Rochester. All publications arising from this report MUST either 1) include Meghan Clark or 2) acknowledge Meghan Clark and the X-ray Crystallographic Facility of the Department of Chemistry at the University of Rochester.

¹ APEX2, version 2009.1-0; Bruker AXS: Madison, WI, 2009.

² Sheldrick, G. M. SADABS, version 2008/1; University of Göttingen: Göttingen, Germany, 2008.

³ SAINT, version 7.60A; Bruker AXS: Madison, WI, 2008.

⁴ Sheldrick, G. M. *Acta Cryst.* **2008**, *A64*, 112-122.

⁵ Altomare, A.; Burla, M. C.; Camalli, M.; Cascarano, G. L.; Giacovazzo, C.; Guagliardi, A.; Moliterni, A. G. G.; Polidori, G.; Spagna, R. *SIR97: A new program for solving and refining crystal structures*; Istituto di Cristallografia, CNR: Bari, Italy, 1999.

⁶ Spek, A. L. *PLATON: A multipurpose crystallographic tool*, version 300106; Utrecht University: Utrecht, The Netherlands, 2006.

Some equations of interest:

$$R_{\text{int}} = \sum |F_o^2 - \langle F_o^2 \rangle| / \sum |F_o^2|$$

$$R1 = \sum |F_o| - |F_c| / \sum |F_o|$$

$$wR2 = [\sum [w(F_o^2 - F_c^2)^2] / \sum [w(F_o^2)^2]]^{1/2}$$

where $w = 1 / [\sigma^2 (F_o^2) + (aP)^2 + bP]$ and

$$P = 1/3 \max(0, F_o^2) + 2/3 F_c^2$$

$$\text{GOF} = S = [\sum [w(F_o^2 - F_c^2)^2] / (m-n)]^{1/2}$$

where m = number of reflections and n = number of parameters

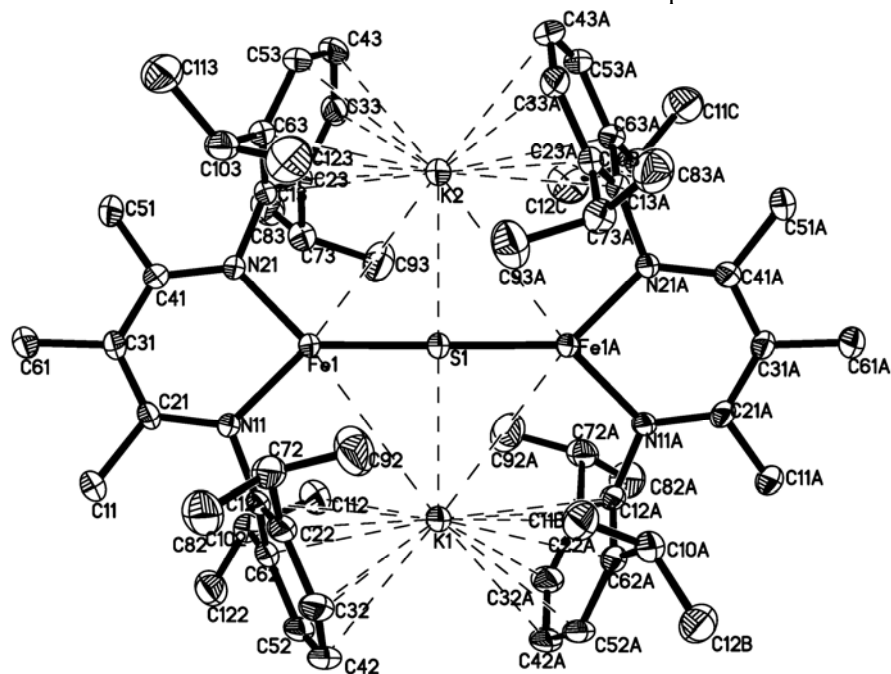


Table 1. Crystal data and structure refinement for holmc10.

Identification code	holmc10		
Empirical formula	C83 H112 Fe2 K2 N4 O0.50 S		
Formula weight	1395.73		
Temperature	100.0(1) K		
Wavelength	0.71073 Å		
Crystal system	Orthorhombic		
Space group	<i>Pbcn</i>		
Unit cell dimensions	<i>a</i> = 14.703(7) Å	α = 90°	
	<i>b</i> = 28.746(14) Å	β = 90°	
	<i>c</i> = 17.341(10) Å	γ = 90°	
Volume	7330(6) Å ³		
<i>Z</i>	4		
Density (calculated)	1.265 Mg/m ³		
Absorption coefficient	0.586 mm ⁻¹		
<i>F</i> (000)	2992		
Crystal color, morphology	Green-black, Block		
Crystal size	0.36 x 0.28 x 0.14 mm ³		
Theta range for data collection	1.84 to 33.14°		
Index ranges	-22 ≤ <i>h</i> ≤ 22, -44 ≤ <i>k</i> ≤ 44, -26 ≤ <i>l</i> ≤ 26		
Reflections collected	133922		
Independent reflections	13994 [<i>R</i> (int) = 0.1062]		
Observed reflections	7828		
Completeness to theta = 33.14°	100.0%		
Absorption correction	Multi-scan		
Max. and min. transmission	0.9225 and 0.8169		
Refinement method	Full-matrix least-squares on <i>F</i> ²		
Data / restraints / parameters	13994 / 0 / 324		
Goodness-of-fit on <i>F</i> ²	1.018		
Final <i>R</i> indices [<i>I</i> >2sigma(<i>I</i>)]	<i>R</i> 1 = 0.0645, <i>wR</i> 2 = 0.1750		
<i>R</i> indices (all data)	<i>R</i> 1 = 0.1057, <i>wR</i> 2 = 0.1921		
Largest diff. peak and hole	0.941 and -0.494 e.Å ⁻³		

Table 2. Atomic coordinates ($x \times 10^4$) and equivalent isotropic displacement parameters ($\text{\AA}^2 \times 10^3$) for holmc10. U_{eq} is defined as one third of the trace of the orthogonalized U_{ij} tensor.

	x	y	z	U_{eq}
Fe1	4802(1)	3089(1)	6257(1)	27(1)
K1	5000	4111(1)	7500	33(1)
K2	5000	2070(1)	7500	32(1)
S1	5000	3091(1)	7500	38(1)
N11	4943(1)	3555(1)	5472(1)	28(1)
N21	4405(1)	2625(1)	5538(1)	25(1)
C11	5067(2)	3900(1)	4185(1)	35(1)
C21	4825(2)	3497(1)	4710(1)	27(1)
C31	4508(2)	3088(1)	4379(1)	24(1)
C41	4285(2)	2678(1)	4776(1)	25(1)
C51	3895(2)	2278(1)	4329(1)	34(1)
C61	4417(2)	3073(1)	3518(1)	33(1)
C12	5163(2)	4002(1)	5749(1)	28(1)
C22	6056(2)	4113(1)	5937(1)	31(1)
C32	6248(2)	4547(1)	6245(1)	34(1)
C42	5578(2)	4872(1)	6359(1)	35(1)
C52	4710(2)	4764(1)	6160(1)	33(1)
C62	4468(2)	4334(1)	5858(1)	31(1)
C72	6824(2)	3778(1)	5789(1)	35(1)
C82	7480(2)	3968(1)	5194(2)	46(1)
C92	7321(2)	3652(1)	6518(2)	60(1)
C102	3496(2)	4218(1)	5687(1)	33(1)
C112	3026(2)	4047(1)	6410(1)	42(1)
C122	2982(2)	4617(1)	5334(1)	43(1)
C13	4284(2)	2173(1)	5851(1)	24(1)
C23	3487(2)	2060(1)	6240(1)	27(1)
C33	3420(2)	1625(1)	6587(1)	31(1)
C43	4110(2)	1306(1)	6536(1)	35(1)
C53	4880(2)	1415(1)	6139(1)	31(1)
C63	4987(2)	1848(1)	5790(1)	28(1)
C73	2702(2)	2392(1)	6291(1)	32(1)

C83	1837(2)	2181(1)	5962(2)	45(1)
C93	2532(2)	2550(1)	7115(2)	48(1)
C103	5861(2)	1964(1)	5391(1)	36(1)
C113	6177(2)	1586(1)	4840(2)	50(1)
C123	6594(2)	2070(1)	5977(2)	52(1)

Table 3. Bond lengths [\AA] and angles [$^\circ$] for holmc10.

Fe(1)-N(21)	1.9166(17)	C(11)-C(21)	1.517(3)
Fe(1)-N(11)	1.9210(18)	C(11)-H(11A)	0.9800
Fe(1)-S(1)	2.1745(13)	C(11)-H(11B)	0.9800
Fe(1)-K(2)	3.6490(14)	C(11)-H(11C)	0.9800
Fe(1)-K(1)	3.6548(14)	C(21)-C(31)	1.388(3)
K(1)-S(1)	2.9318(17)	C(31)-C(41)	1.404(3)
K(1)-C(52)#1	3.017(2)	C(31)-C(61)	1.499(3)
K(1)-C(52)	3.017(2)	C(41)-C(51)	1.502(3)
K(1)-C(62)#1	3.022(2)	C(51)-H(51A)	0.9800
K(1)-C(62)	3.022(2)	C(51)-H(51B)	0.9800
K(1)-C(12)	3.062(3)	C(51)-H(51C)	0.9800
K(1)-C(12)#1	3.062(3)	C(61)-H(61A)	0.9800
K(1)-C(42)#1	3.069(2)	C(61)-H(61B)	0.9800
K(1)-C(42)	3.069(2)	C(61)-H(61C)	0.9800
K(1)-C(32)#1	3.110(2)	C(12)-C(22)	1.390(3)
K(1)-C(32)	3.110(2)	C(12)-C(62)	1.412(3)
K(1)-C(22)#1	3.125(2)	C(22)-C(32)	1.387(3)
K(2)-S(1)	2.9360(17)	C(22)-C(72)	1.506(3)
K(2)-C(53)#1	3.025(2)	C(32)-C(42)	1.372(3)
K(2)-C(53)	3.025(2)	C(32)-H(32A)	0.9500
K(2)-C(63)	3.032(3)	C(42)-C(52)	1.358(4)
K(2)-C(63)#1	3.032(3)	C(42)-H(42A)	0.9500
K(2)-C(43)#1	3.053(2)	C(52)-C(62)	1.391(3)
K(2)-C(43)	3.053(2)	C(52)-H(52A)	0.9500
K(2)-C(13)	3.062(2)	C(62)-C(102)	1.496(4)
K(2)-C(13)#1	3.062(2)	C(72)-C(92)	1.505(4)
K(2)-C(33)#1	3.089(2)	C(72)-C(82)	1.514(3)
K(2)-C(33)	3.089(2)	C(72)-H(72A)	1.0000
K(2)-C(23)#1	3.119(2)	C(82)-H(82A)	0.9800
S(1)-Fe(1)#1	2.1745(13)	C(82)-H(82B)	0.9800
N(11)-C(21)	1.344(3)	C(82)-H(82C)	0.9800
N(11)-C(12)	1.408(3)	C(92)-H(92A)	0.9800
N(21)-C(41)	1.343(2)	C(92)-H(92B)	0.9800
N(21)-C(13)	1.419(2)	C(92)-H(92C)	0.9800

C(102)-C(122)	1.504(3)	C(123)-H(12E)	0.9800
C(102)-C(112)	1.514(3)	C(123)-H(12F)	0.9800
C(102)-H(10A)	1.0000		
C(112)-H(11D)	0.9800	N(21)-Fe(1)-N(11)	93.29(8)
C(112)-H(11E)	0.9800	N(21)-Fe(1)-S(1)	133.41(5)
C(112)-H(11F)	0.9800	N(11)-Fe(1)-S(1)	133.30(6)
C(122)-H(12A)	0.9800	N(21)-Fe(1)-K(2)	81.36(6)
C(122)-H(12B)	0.9800	N(11)-Fe(1)-K(2)	165.88(6)
C(122)-H(12C)	0.9800	S(1)-Fe(1)-K(2)	53.57(3)
C(13)-C(23)	1.392(3)	N(21)-Fe(1)-K(1)	165.25(6)
C(13)-C(63)	1.396(3)	N(11)-Fe(1)-K(1)	81.29(6)
C(23)-C(33)	1.390(3)	S(1)-Fe(1)-K(1)	53.34(3)
C(23)-C(73)	1.499(3)	K(2)-Fe(1)-K(1)	106.91(4)
C(33)-C(43)	1.371(3)	S(1)-K(1)-C(52)#1	128.48(4)
C(33)-H(33A)	0.9500	S(1)-K(1)-C(52)	128.48(4)
C(43)-C(53)	1.362(3)	C(52)#1-K(1)-C(52)	103.04(9)
C(43)-H(43A)	0.9500	S(1)-K(1)-C(62)#1	102.22(4)
C(53)-C(63)	1.394(3)	C(52)#1-K(1)-C(62)#1	26.63(6)
C(53)-H(53A)	0.9500	C(52)-K(1)-C(62)#1	129.09(7)
C(63)-C(103)	1.497(3)	S(1)-K(1)-C(62)	102.22(4)
C(73)-C(83)	1.519(3)	C(52)#1-K(1)-C(62)	129.09(7)
C(73)-C(93)	1.520(3)	C(52)-K(1)-C(62)	26.63(6)
C(73)-H(73A)	1.0000	C(62)#1-K(1)-C(62)	155.57(8)
C(83)-H(83A)	0.9800	S(1)-K(1)-C(12)	84.10(4)
C(83)-H(83B)	0.9800	C(52)#1-K(1)-C(12)	144.71(6)
C(83)-H(83C)	0.9800	C(52)-K(1)-C(12)	46.50(6)
C(93)-H(93A)	0.9800	C(62)#1-K(1)-C(12)	159.38(7)
C(93)-H(93B)	0.9800	C(62)-K(1)-C(12)	26.82(6)
C(93)-H(93C)	0.9800	S(1)-K(1)-C(12)#1	84.10(4)
C(103)-C(123)	1.512(4)	C(52)#1-K(1)-C(12)#1	46.50(6)
C(103)-C(113)	1.519(3)	C(52)-K(1)-C(12)#1	144.71(6)
C(103)-H(10B)	1.0000	C(62)#1-K(1)-C(12)#1	26.82(6)
C(113)-H(11G)	0.9800	C(62)-K(1)-C(12)#1	159.38(7)
C(113)-H(11H)	0.9800	C(12)-K(1)-C(12)#1	168.20(7)
C(113)-H(11I)	0.9800	S(1)-K(1)-C(42)#1	135.43(5)
C(123)-H(12D)	0.9800	C(52)#1-K(1)-C(42)#1	25.77(7)

C(52)-K(1)-C(42)#1	90.80(7)	C(62)-K(1)-C(22)#1	133.52(7)
C(62)#1-K(1)-C(42)#1	46.63(7)	C(12)-K(1)-C(22)#1	154.10(7)
C(62)-K(1)-C(42)#1	112.66(7)	C(12)#1-K(1)-C(22)#1	25.94(6)
C(12)-K(1)-C(42)#1	137.25(6)	C(42)#1-K(1)-C(22)#1	45.71(6)
C(12)#1-K(1)-C(42)#1	53.99(6)	C(42)-K(1)-C(22)#1	134.11(6)
S(1)-K(1)-C(42)	135.43(5)	C(32)#1-K(1)-C(22)#1	25.70(5)
C(52)#1-K(1)-C(42)	90.80(7)	C(32)-K(1)-C(22)#1	154.14(6)
C(52)-K(1)-C(42)	25.77(7)	S(1)-K(2)-C(53)#1	128.50(4)
C(62)#1-K(1)-C(42)	112.66(7)	S(1)-K(2)-C(53)	128.50(4)
C(62)-K(1)-C(42)	46.62(7)	C(53)#1-K(2)-C(53)	103.01(9)
C(12)-K(1)-C(42)	53.99(6)	S(1)-K(2)-C(63)	102.12(4)
C(12)#1-K(1)-C(42)	137.25(6)	C(53)#1-K(2)-C(63)	129.25(7)
C(42)#1-K(1)-C(42)	89.14(9)	C(53)-K(2)-C(63)	26.61(5)
S(1)-K(1)-C(32)#1	113.75(4)	S(1)-K(2)-C(63)#1	102.12(4)
C(52)#1-K(1)-C(32)#1	45.11(7)	C(53)#1-K(2)-C(63)#1	26.61(5)
C(52)-K(1)-C(32)#1	101.80(7)	C(53)-K(2)-C(63)#1	129.26(7)
C(62)#1-K(1)-C(32)#1	53.72(7)	C(63)-K(2)-C(63)#1	155.76(8)
C(62)-K(1)-C(32)#1	114.92(7)	S(1)-K(2)-C(43)#1	135.97(5)
C(12)-K(1)-C(32)#1	141.40(7)	C(53)#1-K(2)-C(43)#1	25.90(6)
C(12)#1-K(1)-C(32)#1	45.67(6)	C(53)-K(2)-C(43)#1	90.26(7)
C(42)#1-K(1)-C(32)#1	25.65(6)	C(63)-K(2)-C(43)#1	112.75(6)
C(42)-K(1)-C(32)#1	109.13(7)	C(63)#1-K(2)-C(43)#1	46.48(6)
S(1)-K(1)-C(32)	113.75(4)	S(1)-K(2)-C(43)	135.97(5)
C(52)#1-K(1)-C(32)	101.80(7)	C(53)#1-K(2)-C(43)	90.25(7)
C(52)-K(1)-C(32)	45.11(7)	C(53)-K(2)-C(43)	25.90(7)
C(62)#1-K(1)-C(32)	114.92(7)	C(63)-K(2)-C(43)	46.48(6)
C(62)-K(1)-C(32)	53.72(7)	C(63)#1-K(2)-C(43)	112.75(6)
C(12)-K(1)-C(32)	45.67(6)	C(43)#1-K(2)-C(43)	88.05(9)
C(12)#1-K(1)-C(32)	141.40(7)	S(1)-K(2)-C(13)	84.43(4)
C(42)#1-K(1)-C(32)	109.13(7)	C(53)#1-K(2)-C(13)	144.04(6)
C(42)-K(1)-C(32)	25.65(6)	C(53)-K(2)-C(13)	46.48(6)
C(32)#1-K(1)-C(32)	132.51(9)	C(63)-K(2)-C(13)	26.49(6)
S(1)-K(1)-C(22)#1	90.09(4)	C(63)#1-K(2)-C(13)	159.35(6)
C(52)#1-K(1)-C(22)#1	53.23(7)	C(43)#1-K(2)-C(13)	136.73(6)
C(52)-K(1)-C(22)#1	126.63(7)	C(43)-K(2)-C(13)	53.94(6)
C(62)#1-K(1)-C(22)#1	46.42(7)	S(1)-K(2)-C(13)#1	84.43(4)

C(53)#1-K(2)-C(13)#1	46.48(6)	C(33)-K(2)-C(23)#1	153.17(6)
C(53)-K(2)-C(13)#1	144.04(6)	Fe(1)#1-S(1)-Fe(1)	179.70(4)
C(63)-K(2)-C(13)#1	159.36(6)	Fe(1)#1-S(1)-K(1)	90.15(2)
C(63)#1-K(2)-C(13)#1	26.49(6)	Fe(1)-S(1)-K(1)	90.15(2)
C(43)#1-K(2)-C(13)#1	53.95(6)	Fe(1)#1-S(1)-K(2)	89.85(2)
C(43)-K(2)-C(13)#1	136.73(6)	Fe(1)-S(1)-K(2)	89.85(2)
C(13)-K(2)-C(13)#1	168.86(7)	K(1)-S(1)-K(2)	180.0
S(1)-K(2)-C(33)#1	114.43(4)	C(21)-N(11)-C(12)	118.59(16)
C(53)#1-K(2)-C(33)#1	45.45(7)	C(21)-N(11)-Fe(1)	126.58(14)
C(53)-K(2)-C(33)#1	100.75(6)	C(12)-N(11)-Fe(1)	114.80(13)
C(63)-K(2)-C(33)#1	114.79(6)	C(41)-N(21)-C(13)	117.61(15)
C(63)#1-K(2)-C(33)#1	53.64(6)	C(41)-N(21)-Fe(1)	126.97(13)
C(43)#1-K(2)-C(33)#1	25.80(6)	C(13)-N(21)-Fe(1)	115.29(12)
C(43)-K(2)-C(33)#1	107.79(7)	C(21)-C(11)-H(11A)	109.5
C(13)-K(2)-C(33)#1	141.05(6)	C(21)-C(11)-H(11B)	109.5
C(13)#1-K(2)-C(33)#1	45.79(5)	H(11A)-C(11)-H(11B)	109.5
S(1)-K(2)-C(33)	114.43(4)	C(21)-C(11)-H(11C)	109.5
C(53)#1-K(2)-C(33)	100.75(6)	H(11A)-C(11)-H(11C)	109.5
C(53)-K(2)-C(33)	45.45(7)	H(11B)-C(11)-H(11C)	109.5
C(63)-K(2)-C(33)	53.63(6)	N(11)-C(21)-C(31)	123.81(17)
C(63)#1-K(2)-C(33)	114.79(6)	N(11)-C(21)-C(11)	117.69(18)
C(43)#1-K(2)-C(33)	107.79(7)	C(31)-C(21)-C(11)	118.49(17)
C(43)-K(2)-C(33)	25.79(6)	C(21)-C(31)-C(41)	125.83(17)
C(13)-K(2)-C(33)	45.79(5)	C(21)-C(31)-C(61)	117.87(17)
C(13)#1-K(2)-C(33)	141.05(6)	C(41)-C(31)-C(61)	116.28(17)
C(33)#1-K(2)-C(33)	131.13(9)	N(21)-C(41)-C(31)	123.24(17)
S(1)-K(2)-C(23)#1	90.51(4)	N(21)-C(41)-C(51)	118.07(17)
C(53)#1-K(2)-C(23)#1	53.57(6)	C(31)-C(41)-C(51)	118.69(17)
C(53)-K(2)-C(23)#1	125.65(6)	C(41)-C(51)-H(51A)	109.5
C(63)-K(2)-C(23)#1	133.44(6)	C(41)-C(51)-H(51B)	109.5
C(63)#1-K(2)-C(23)#1	46.27(6)	H(51A)-C(51)-H(51B)	109.5
C(43)#1-K(2)-C(23)#1	45.94(6)	C(41)-C(51)-H(51C)	109.5
C(43)-K(2)-C(23)#1	133.05(6)	H(51A)-C(51)-H(51C)	109.5
C(13)-K(2)-C(23)#1	154.21(6)	H(51B)-C(51)-H(51C)	109.5
C(13)#1-K(2)-C(23)#1	26.01(6)	C(31)-C(61)-H(61A)	109.5
C(33)#1-K(2)-C(23)#1	25.88(5)	C(31)-C(61)-H(61B)	109.5

H(61A)-C(61)-H(61B)	109.5	C(12)-C(62)-C(102)	120.99(19)
C(31)-C(61)-H(61C)	109.5	C(52)-C(62)-K(1)	76.52(12)
H(61A)-C(61)-H(61C)	109.5	C(12)-C(62)-K(1)	78.20(11)
H(61B)-C(61)-H(61C)	109.5	C(102)-C(62)-K(1)	112.76(12)
C(22)-C(12)-N(11)	120.46(19)	C(92)-C(72)-C(22)	111.96(19)
C(22)-C(12)-C(62)	119.84(19)	C(92)-C(72)-C(82)	110.5(3)
N(11)-C(12)-C(62)	119.7(2)	C(22)-C(72)-C(82)	111.3(2)
C(22)-C(12)-K(1)	79.53(11)	C(92)-C(72)-H(72A)	107.6
N(11)-C(12)-K(1)	114.40(11)	C(22)-C(72)-H(72A)	107.6
C(62)-C(12)-K(1)	74.98(11)	C(82)-C(72)-H(72A)	107.6
C(32)-C(22)-C(12)	119.3(2)	C(72)-C(82)-H(82A)	109.5
C(32)-C(22)-C(72)	119.3(2)	C(72)-C(82)-H(82B)	109.5
C(12)-C(22)-C(72)	121.38(19)	H(82A)-C(82)-H(82B)	109.5
C(32)-C(22)-K(1)	76.58(12)	C(72)-C(82)-H(82C)	109.5
C(12)-C(22)-K(1)	74.53(11)	H(82A)-C(82)-H(82C)	109.5
C(72)-C(22)-K(1)	121.29(13)	H(82B)-C(82)-H(82C)	109.5
C(42)-C(32)-C(22)	121.4(2)	C(72)-C(92)-H(92A)	109.5
C(42)-C(32)-K(1)	75.47(13)	C(72)-C(92)-H(92B)	109.5
C(22)-C(32)-K(1)	77.72(12)	H(92A)-C(92)-H(92B)	109.5
C(42)-C(32)-H(32A)	119.3	C(72)-C(92)-H(92C)	109.5
C(22)-C(32)-H(32A)	119.3	H(92A)-C(92)-H(92C)	109.5
K(1)-C(32)-H(32A)	118.3	H(92B)-C(92)-H(92C)	109.5
C(52)-C(42)-C(32)	119.0(2)	C(62)-C(102)-C(122)	113.1(2)
C(52)-C(42)-K(1)	75.01(12)	C(62)-C(102)-C(112)	110.11(19)
C(32)-C(42)-K(1)	78.88(12)	C(122)-C(102)-C(112)	110.8(2)
C(52)-C(42)-H(42A)	120.5	C(62)-C(102)-H(10A)	107.6
C(32)-C(42)-H(42A)	120.5	C(122)-C(102)-H(10A)	107.6
K(1)-C(42)-H(42A)	116.4	C(112)-C(102)-H(10A)	107.6
C(42)-C(52)-C(62)	122.6(2)	C(102)-C(112)-H(11D)	109.5
C(42)-C(52)-K(1)	79.22(13)	C(102)-C(112)-H(11E)	109.5
C(62)-C(52)-K(1)	76.85(12)	H(11D)-C(112)-H(11E)	109.5
C(42)-C(52)-H(52A)	118.7	C(102)-C(112)-H(11F)	109.5
C(62)-C(52)-H(52A)	118.7	H(11D)-C(112)-H(11F)	109.5
K(1)-C(52)-H(52A)	115.5	H(11E)-C(112)-H(11F)	109.5
C(52)-C(62)-C(12)	117.8(2)	C(102)-C(122)-H(12A)	109.5
C(52)-C(62)-C(102)	121.1(2)	C(102)-C(122)-H(12B)	109.5

H(12A)-C(122)-H(12B)	109.5	C(13)-C(63)-C(103)	121.43(18)
C(102)-C(122)-H(12C)	109.5	C(53)-C(63)-K(2)	76.39(12)
H(12A)-C(122)-H(12C)	109.5	C(13)-C(63)-K(2)	77.95(11)
H(12B)-C(122)-H(12C)	109.5	C(103)-C(63)-K(2)	113.59(15)
C(23)-C(13)-C(63)	120.23(18)	C(23)-C(73)-C(83)	111.6(2)
C(23)-C(13)-N(21)	120.26(18)	C(23)-C(73)-C(93)	111.83(19)
C(63)-C(13)-N(21)	119.46(19)	C(83)-C(73)-C(93)	109.5(2)
C(23)-C(13)-K(2)	79.25(11)	C(23)-C(73)-H(73A)	107.9
C(63)-C(13)-K(2)	75.56(11)	C(83)-C(73)-H(73A)	107.9
N(21)-C(13)-K(2)	113.73(11)	C(93)-C(73)-H(73A)	107.9
C(33)-C(23)-C(13)	118.6(2)	C(73)-C(83)-H(83A)	109.5
C(33)-C(23)-C(73)	119.5(2)	C(73)-C(83)-H(83B)	109.5
C(13)-C(23)-C(73)	121.91(18)	H(83A)-C(83)-H(83B)	109.5
C(33)-C(23)-K(2)	75.86(12)	C(73)-C(83)-H(83C)	109.5
C(13)-C(23)-K(2)	74.73(12)	H(83A)-C(83)-H(83C)	109.5
C(73)-C(23)-K(2)	120.16(13)	H(83B)-C(83)-H(83C)	109.5
C(43)-C(33)-C(23)	121.5(2)	C(73)-C(93)-H(93A)	109.5
C(43)-C(33)-K(2)	75.66(13)	C(73)-C(93)-H(93B)	109.5
C(23)-C(33)-K(2)	78.26(12)	H(93A)-C(93)-H(93B)	109.5
C(43)-C(33)-H(33A)	119.3	C(73)-C(93)-H(93C)	109.5
C(23)-C(33)-H(33A)	119.3	H(93A)-C(93)-H(93C)	109.5
K(2)-C(33)-H(33A)	117.5	H(93B)-C(93)-H(93C)	109.5
C(53)-C(43)-C(33)	119.59(19)	C(63)-C(103)-C(123)	110.3(2)
C(53)-C(43)-K(2)	75.87(13)	C(63)-C(103)-C(113)	113.3(2)
C(33)-C(43)-K(2)	78.54(13)	C(123)-C(103)-C(113)	110.4(2)
C(53)-C(43)-H(43A)	120.2	C(63)-C(103)-H(10B)	107.5
C(33)-C(43)-H(43A)	120.2	C(123)-C(103)-H(10B)	107.5
K(2)-C(43)-H(43A)	116.1	C(113)-C(103)-H(10B)	107.5
C(43)-C(53)-C(63)	121.2(2)	C(103)-C(113)-H(11G)	109.5
C(43)-C(53)-K(2)	78.23(13)	C(103)-C(113)-H(11H)	109.5
C(63)-C(53)-K(2)	77.01(12)	H(11G)-C(113)-H(11H)	109.5
C(43)-C(53)-H(53A)	119.4	C(103)-C(113)-H(11I)	109.5
C(63)-C(53)-H(53A)	119.4	H(11G)-C(113)-H(11I)	109.5
K(2)-C(53)-H(53A)	115.9	H(11H)-C(113)-H(11I)	109.5
C(53)-C(63)-C(13)	118.8(2)	C(103)-C(123)-H(12D)	109.5
C(53)-C(63)-C(103)	119.7(2)	C(103)-C(123)-H(12E)	109.5

H(12D)-C(123)-H(12E)	109.5	H(12D)-C(123)-H(12F)	109.5
C(103)-C(123)-H(12F)	109.5	H(12E)-C(123)-H(12F)	109.5

Symmetry transformations used to generate equivalent atoms:

#1 -x+1,y,-z+3/2

Table 4. Anisotropic displacement parameters ($\text{\AA}^2 \times 10^3$) for holmc10. The anisotropic displacement factor exponent takes the form: $-2\pi^2 [h^2 a^{*2} U_{11} + \dots + 2 h k a^{*} b^{*} U_{12}]$

	U_{11}	U_{22}	U_{33}	U_{23}	U_{13}	U_{12}
Fe1	53(1)	15(1)	13(1)	0(1)	3(1)	-2(1)
K1	62(1)	19(1)	17(1)	0	4(1)	0
K2	54(1)	21(1)	20(1)	0	-9(1)	0
S1	81(1)	18(1)	14(1)	0	1(1)	0
N11	53(1)	16(1)	14(1)	-1(1)	6(1)	0(1)
N21	44(1)	17(1)	14(1)	0(1)	1(1)	-1(1)
C11	59(2)	25(1)	19(1)	5(1)	4(1)	-1(1)
C21	44(1)	22(1)	15(1)	4(1)	5(1)	5(1)
C31	35(1)	23(1)	15(1)	3(1)	0(1)	4(1)
C41	36(1)	19(1)	19(1)	-1(1)	1(1)	2(1)
C51	55(2)	29(1)	18(1)	-1(1)	-4(1)	-4(1)
C61	53(1)	27(1)	20(1)	3(1)	-3(1)	-7(1)
C12	50(1)	17(1)	16(1)	3(1)	8(1)	-2(1)
C22	51(1)	20(1)	22(1)	1(1)	11(1)	-2(1)
C32	51(1)	21(1)	32(1)	1(1)	9(1)	-7(1)
C42	59(2)	15(1)	31(1)	0(1)	4(1)	-6(1)
C52	58(2)	14(1)	27(1)	1(1)	7(1)	5(1)
C62	56(1)	20(1)	16(1)	3(1)	5(1)	1(1)
C72	50(1)	27(1)	28(1)	-2(1)	16(1)	-1(1)
C82	50(2)	48(2)	40(1)	4(1)	16(1)	-2(1)
C92	85(2)	57(2)	36(1)	6(1)	14(1)	32(2)
C102	52(2)	26(1)	22(1)	-1(1)	2(1)	1(1)
C112	54(2)	40(1)	31(1)	5(1)	4(1)	-7(1)
C122	56(2)	39(1)	34(1)	5(1)	4(1)	11(1)
C13	41(1)	18(1)	15(1)	1(1)	-3(1)	-2(1)
C23	42(1)	22(1)	17(1)	0(1)	-3(1)	-3(1)
C33	42(1)	28(1)	23(1)	3(1)	-4(1)	-10(1)
C43	56(2)	19(1)	28(1)	6(1)	-7(1)	-8(1)
C53	52(1)	16(1)	25(1)	0(1)	-5(1)	2(1)
C63	47(1)	18(1)	20(1)	-1(1)	1(1)	-1(1)
C73	41(1)	30(1)	26(1)	2(1)	1(1)	-2(1)

C83	44(2)	47(2)	43(1)	6(1)	-10(1)	-3(1)
C93	51(2)	58(2)	35(1)	-10(1)	-1(1)	7(1)
C103	52(2)	24(1)	32(1)	2(1)	11(1)	6(1)
C113	64(2)	40(1)	45(1)	-2(1)	19(1)	15(1)
C123	47(2)	55(2)	54(2)	-4(1)	9(1)	-10(1)

Table 5. Hydrogen coordinates ($x \times 10^4$) and isotropic displacement parameters ($\text{\AA}^2 \times 10^3$) for holmc10.

	x	y	z	U(eq)
H11A	5284	4162	4497	52
H11B	4527	3995	3894	52
H11C	5546	3804	3826	52
H51A	3566	2071	4681	51
H51B	4389	2105	4080	51
H51C	3476	2396	3936	51
H61A	4850	3290	3285	50
H61B	3797	3161	3372	50
H61C	4544	2757	3335	50
H32A	6858	4621	6380	41
H42A	5719	5167	6573	42
H52A	4249	4992	6231	39
H72A	6554	3486	5575	42
H82A	7154	4026	4710	69
H82B	7966	3741	5103	69
H82C	7745	4259	5383	69
H92A	6896	3507	6882	89
H92B	7577	3934	6750	89
H92C	7812	3433	6399	89
H10A	3494	3956	5306	40
H11D	3343	3772	6607	63
H11E	2394	3966	6290	63
H11F	3036	4293	6802	63
H12A	3294	4720	4865	65
H12B	2952	4874	5702	65
H12C	2364	4515	5204	65
H33A	2884	1548	6864	37
H43A	4052	1011	6778	41
H53A	5353	1191	6098	37
H73A	2856	2673	5977	39

H83A	1936	2097	5421	67
H83B	1342	2408	5998	67
H83C	1677	1902	6256	67
H93A	3068	2715	7308	72
H93B	2412	2278	7441	72
H93C	2004	2758	7127	72
H10B	5757	2252	5081	43
H11G	6720	1693	4564	75
H11H	5692	1518	4469	75
H11I	6323	1304	5132	75
H12D	6408	2337	6292	78
H12E	7163	2144	5709	78
H12F	6687	1799	6309	78

Table 6. Torsion angles [°] for holmc10.

N21-Fe1-S1-Fe1#1	17(18)	C62#1-K1-S1-K2	-75(24)
N11-Fe1-S1-Fe1#1	-164(18)	C62-K1-S1-K2	105(24)
K2-Fe1-S1-Fe1#1	0(18)	C12-K1-S1-K2	85(24)
K1-Fe1-S1-Fe1#1	180(18)	C12#1-K1-S1-K2	-95(24)
N21-Fe1-S1-K1	-162.81(8)	C42#1-K1-S1-K2	-113(24)
N11-Fe1-S1-K1	16.13(8)	C42-K1-S1-K2	67(24)
K2-Fe1-S1-K1	180.0	C32#1-K1-S1-K2	-130(24)
N21-Fe1-S1-K2	17.19(8)	C32-K1-S1-K2	50(24)
N11-Fe1-S1-K2	-163.87(8)	C22#1-K1-S1-K2	-120(24)
K1-Fe1-S1-K2	180.0	C53#1-K2-S1-Fe1#1	3.44(6)
C52#1-K1-S1-Fe1#1	2.71(6)	C53-K2-S1-Fe1#1	-176.56(6)
C52-K1-S1-Fe1#1	-177.29(6)	C63-K2-S1-Fe1#1	-172.66(5)
C62#1-K1-S1-Fe1#1	7.66(5)	C63#1-K2-S1-Fe1#1	7.34(5)
C62-K1-S1-Fe1#1	-172.34(5)	C43#1-K2-S1-Fe1#1	-30.36(7)
C12-K1-S1-Fe1#1	167.77(5)	C43-K2-S1-Fe1#1	149.64(7)
C12#1-K1-S1-Fe1#1	-12.23(5)	C13-K2-S1-Fe1#1	167.51(4)
C42#1-K1-S1-Fe1#1	-30.94(8)	C13#1-K2-S1-Fe1#1	-12.49(4)
C42-K1-S1-Fe1#1	149.06(8)	C33#1-K2-S1-Fe1#1	-48.02(5)
C32#1-K1-S1-Fe1#1	-47.85(6)	C33-K2-S1-Fe1#1	131.99(5)
C32-K1-S1-Fe1#1	132.15(6)	C23#1-K2-S1-Fe1#1	-37.82(4)
C22#1-K1-S1-Fe1#1	-37.51(5)	C53#1-K2-S1-Fe1	-176.56(6)
C52#1-K1-S1-Fe1	-177.29(6)	C53-K2-S1-Fe1	3.44(6)
C52-K1-S1-Fe1	2.71(6)	C63-K2-S1-Fe1	7.34(5)
C62#1-K1-S1-Fe1	-172.34(5)	C63#1-K2-S1-Fe1	-172.66(5)
C62-K1-S1-Fe1	7.66(5)	C43#1-K2-S1-Fe1	149.64(7)
C12-K1-S1-Fe1	-12.23(5)	C43-K2-S1-Fe1	-30.36(7)
C12#1-K1-S1-Fe1	167.77(5)	C13-K2-S1-Fe1	-12.49(4)
C42#1-K1-S1-Fe1	149.06(8)	C13#1-K2-S1-Fe1	167.51(4)
C42-K1-S1-Fe1	-30.94(8)	C33#1-K2-S1-Fe1	131.99(5)
C32#1-K1-S1-Fe1	132.15(6)	C33-K2-S1-Fe1	-48.01(5)
C32-K1-S1-Fe1	-47.85(6)	C23#1-K2-S1-Fe1	142.18(4)
C22#1-K1-S1-Fe1	142.49(5)	C53#1-K2-S1-K1	86(25)
C52#1-K1-S1-K2	-80(24)	C53-K2-S1-K1	-94(24)
C52-K1-S1-K2	100(24)	C63-K2-S1-K1	-90(25)

C63#1-K2-S1-K1	90(25)	C21-C31-C41-N21	-3.9(4)
C43#1-K2-S1-K1	52(25)	C61-C31-C41-N21	174.2(2)
C43-K2-S1-K1	-128(25)	C21-C31-C41-C51	176.2(2)
C13-K2-S1-K1	-110(25)	C61-C31-C41-C51	-5.7(3)
C13#1-K2-S1-K1	70(25)	C21-N11-C12-C22	-100.5(2)
C33#1-K2-S1-K1	34(25)	Fe1-N11-C12-C22	81.5(2)
C33-K2-S1-K1	-146(25)	C21-N11-C12-C62	81.4(2)
C23#1-K2-S1-K1	44(25)	Fe1-N11-C12-C62	-96.59(19)
N21-Fe1-N11-C21	-3.5(2)	C21-N11-C12-K1	167.45(16)
S1-Fe1-N11-C21	177.28(15)	Fe1-N11-C12-K1	-10.55(19)
K2-Fe1-N11-C21	63.6(4)	S1-K1-C12-C22	-102.48(11)
K1-Fe1-N11-C21	-169.7(2)	C52#1-K1-C12-C22	57.07(17)
N21-Fe1-N11-C12	174.33(16)	C52-K1-C12-C22	93.68(14)
S1-Fe1-N11-C12	-4.9(2)	C62#1-K1-C12-C22	6.8(2)
K2-Fe1-N11-C12	-118.5(2)	C62-K1-C12-C22	125.00(18)
K1-Fe1-N11-C12	8.13(15)	C12#1-K1-C12-C22	-102.48(11)
N11-Fe1-N21-C41	-1.54(19)	C42#1-K1-C12-C22	96.89(15)
S1-Fe1-N21-C41	177.69(14)	C42-K1-C12-C22	61.36(12)
K2-Fe1-N21-C41	-168.40(19)	C32#1-K1-C12-C22	136.22(13)
K1-Fe1-N21-C41	66.3(3)	C32-K1-C12-C22	29.34(11)
N11-Fe1-N21-C13	174.16(16)	C22#1-K1-C12-C22	179.60(17)
S1-Fe1-N21-C13	-6.61(19)	S1-K1-C12-N11	16.36(15)
K2-Fe1-N21-C13	7.30(14)	C52#1-K1-C12-N11	175.90(14)
K1-Fe1-N21-C13	-118.02(19)	C52-K1-C12-N11	-147.5(2)
C12-N11-C21-C31	-172.4(2)	C62#1-K1-C12-N11	125.60(18)
Fe1-N11-C21-C31	5.3(3)	C62-K1-C12-N11	-116.2(2)
C12-N11-C21-C11	8.4(3)	C12#1-K1-C12-N11	16.36(15)
Fe1-N11-C21-C11	-173.86(16)	C42#1-K1-C12-N11	-144.27(15)
N11-C21-C31-C41	-1.5(4)	C42-K1-C12-N11	-179.80(19)
C11-C21-C31-C41	177.6(2)	C32#1-K1-C12-N11	-104.94(16)
N11-C21-C31-C61	-179.6(2)	C32-K1-C12-N11	148.18(19)
C11-C21-C31-C61	-0.4(3)	C22#1-K1-C12-N11	-61.6(2)
C13-N21-C41-C31	-170.6(2)	S1-K1-C12-C62	132.52(13)
Fe1-N21-C41-C31	5.0(3)	C52#1-K1-C12-C62	-67.93(18)
C13-N21-C41-C51	9.3(3)	C52-K1-C12-C62	-31.32(13)
Fe1-N21-C41-C51	-175.10(16)	C62#1-K1-C12-C62	-118.2(2)

C12#1-K1-C12-C62	132.52(13)	S1-K1-C22-C72	-41.43(17)
C42#1-K1-C12-C62	-28.11(17)	C52#1-K1-C22-C72	99.52(18)
C42-K1-C12-C62	-63.64(14)	C52-K1-C22-C72	177.7(2)
C32#1-K1-C12-C62	11.22(17)	C62#1-K1-C22-C72	65.62(19)
C32-K1-C12-C62	-95.66(15)	C62-K1-C22-C72	-148.3(2)
C22#1-K1-C12-C62	54.60(19)	C12-K1-C22-C72	-117.7(2)
N11-C12-C22-C32	-176.69(18)	C12#1-K1-C22-C72	35.2(2)
C62-C12-C22-C32	1.4(3)	C42#1-K1-C22-C72	132.15(17)
K1-C12-C22-C32	-64.43(18)	C42-K1-C22-C72	145.0(2)
N11-C12-C22-C72	5.3(3)	C32#1-K1-C22-C72	160.69(17)
C62-C12-C22-C72	-176.66(18)	C32-K1-C22-C72	116.3(3)
K1-C12-C22-C72	117.54(18)	C22#1-K1-C22-C72	139(16)
N11-C12-C22-K1	-112.26(16)	C12-C22-C32-C42	-0.9(3)
C62-C12-C22-K1	65.80(16)	C72-C22-C32-C42	177.13(19)
S1-K1-C22-C32	-157.73(15)	K1-C22-C32-C42	-64.29(19)
C52#1-K1-C22-C32	-16.78(18)	C12-C22-C32-K1	63.35(17)
C52-K1-C22-C32	61.40(15)	C72-C22-C32-K1	-118.57(18)
C62#1-K1-C22-C32	-50.67(17)	S1-K1-C32-C42	151.86(13)
C62-K1-C22-C32	95.37(16)	C52#1-K1-C32-C42	-66.28(15)
C12-K1-C22-C32	126.0(2)	C52-K1-C32-C42	30.44(13)
C12#1-K1-C22-C32	-81.15(19)	C62#1-K1-C32-C42	-90.80(15)
C42#1-K1-C22-C32	15.85(19)	C62-K1-C32-C42	63.93(15)
C42-K1-C22-C32	28.71(14)	C12-K1-C32-C42	97.78(17)
C32#1-K1-C22-C32	44.4(3)	C12#1-K1-C32-C42	-96.35(17)
C22#1-K1-C22-C32	23(16)	C42#1-K1-C32-C42	-40.62(19)
S1-K1-C22-C12	76.22(11)	C32#1-K1-C32-C42	-28.14(13)
C52#1-K1-C22-C12	-142.83(12)	C22#1-K1-C32-C42	-52.4(2)
C52-K1-C22-C12	-64.65(13)	S1-K1-C32-C22	24.45(16)
C62#1-K1-C22-C12	-176.72(11)	C52#1-K1-C32-C22	166.31(15)
C62-K1-C22-C12	-30.68(11)	C52-K1-C32-C22	-96.96(17)
C12#1-K1-C22-C12	152.81(18)	C62#1-K1-C32-C22	141.80(14)
C42#1-K1-C22-C12	-110.20(13)	C62-K1-C32-C22	-63.47(15)
C42-K1-C22-C12	-97.34(15)	C12-K1-C32-C22	-29.63(13)
C32#1-K1-C22-C12	-81.66(19)	C12#1-K1-C32-C22	136.24(14)
C32-K1-C22-C12	-126.0(2)	C42#1-K1-C32-C22	-168.02(14)
C22#1-K1-C22-C12	-104(16)	C42-K1-C32-C22	-127.4(2)

C32#1-K1-C32-C22	-155.55(16)	C32-K1-C52-C42	-30.30(12)
C22#1-K1-C32-C22	-179.84(7)	C22#1-K1-C52-C42	117.06(14)
C22-C32-C42-C52	-0.3(3)	S1-K1-C52-C62	10.84(17)
K1-C32-C42-C52	-65.78(19)	C52#1-K1-C52-C62	-169.16(17)
C22-C32-C42-K1	65.43(19)	C62#1-K1-C52-C62	-175.40(7)
S1-K1-C42-C52	86.37(14)	C12-K1-C52-C62	31.55(14)
C52#1-K1-C42-C52	-119.34(13)	C12#1-K1-C52-C62	-142.80(14)
C62#1-K1-C42-C52	-134.99(13)	C42#1-K1-C52-C62	-146.27(15)
C62-K1-C42-C52	29.35(12)	C42-K1-C52-C62	127.4(2)
C12-K1-C42-C52	63.14(13)	C32#1-K1-C52-C62	-122.92(15)
C12#1-K1-C42-C52	-121.67(13)	C32-K1-C52-C62	97.07(16)
C42#1-K1-C42-C52	-93.63(14)	C22#1-K1-C52-C62	-115.57(15)
C32#1-K1-C42-C52	-77.26(14)	C42-C52-C62-C12	-0.8(3)
C32-K1-C42-C52	124.3(2)	K1-C52-C62-C12	-68.63(16)
C22#1-K1-C42-C52	-84.46(15)	C42-C52-C62-C102	176.52(19)
S1-K1-C42-C32	-37.96(17)	K1-C52-C62-C102	108.67(17)
C52#1-K1-C42-C32	116.33(15)	C42-C52-C62-K1	67.86(19)
C52-K1-C42-C32	-124.3(2)	C22-C12-C62-C52	-0.5(3)
C62#1-K1-C42-C32	100.68(15)	N11-C12-C62-C52	177.53(17)
C62-K1-C42-C32	-94.99(16)	K1-C12-C62-C52	67.68(16)
C12-K1-C42-C32	-61.19(14)	C22-C12-C62-C102	-177.84(18)
C12#1-K1-C42-C32	114.00(14)	N11-C12-C62-C102	0.2(3)
C42#1-K1-C42-C32	142.04(17)	K1-C12-C62-C102	-109.61(17)
C32#1-K1-C42-C32	158.41(10)	C22-C12-C62-K1	-68.23(16)
C22#1-K1-C42-C32	151.21(13)	N11-C12-C62-K1	109.84(16)
C32-C42-C52-C62	1.2(3)	S1-K1-C62-C52	-171.34(14)
K1-C42-C52-C62	-66.66(19)	C52#1-K1-C62-C52	13.7(2)
C32-C42-C52-K1	67.88(19)	C62#1-K1-C62-C52	8.66(14)
S1-K1-C52-C42	-116.53(12)	C12-K1-C62-C52	-122.7(2)
C52#1-K1-C52-C42	63.47(12)	C12#1-K1-C62-C52	82.6(2)
C62#1-K1-C52-C42	57.23(15)	C42#1-K1-C62-C52	36.99(16)
C62-K1-C52-C42	-127.4(2)	C42-K1-C62-C52	-28.38(14)
C12-K1-C52-C42	-95.82(15)	C32#1-K1-C62-C52	64.96(16)
C12#1-K1-C52-C42	89.83(17)	C32-K1-C62-C52	-60.72(14)
C42#1-K1-C52-C42	86.36(15)	C22#1-K1-C62-C52	86.67(16)
C32#1-K1-C52-C42	109.71(14)	S1-K1-C62-C12	-48.60(13)

C52#1-K1-C62-C12	136.39(12)	C41-N21-C13-K2	166.71(15)
C52-K1-C62-C12	122.7(2)	Fe1-N21-C13-K2	-9.41(18)
C62#1-K1-C62-C12	131.40(13)	S1-K2-C13-C23	-102.72(11)
C12#1-K1-C62-C12	-154.68(17)	C53#1-K2-C13-C23	55.82(16)
C42#1-K1-C62-C12	159.73(12)	C53-K2-C13-C23	94.51(13)
C42-K1-C62-C12	94.36(16)	C63-K2-C13-C23	125.32(18)
C32#1-K1-C62-C12	-172.30(12)	C63#1-K2-C13-C23	7.1(2)
C32-K1-C62-C12	62.02(13)	C43#1-K2-C13-C23	95.40(14)
C22#1-K1-C62-C12	-150.60(12)	C43-K2-C13-C23	61.99(12)
S1-K1-C62-C102	70.27(14)	C13#1-K2-C13-C23	-102.72(11)
C52#1-K1-C62-C102	-104.74(15)	C33#1-K2-C13-C23	134.57(13)
C52-K1-C62-C102	-118.4(2)	C33-K2-C13-C23	29.71(11)
C62#1-K1-C62-C102	-109.73(14)	C23#1-K2-C13-C23	177.72(17)
C12-K1-C62-C102	118.9(2)	S1-K2-C13-C63	131.96(12)
C12#1-K1-C62-C102	-35.8(2)	C53#1-K2-C13-C63	-69.50(17)
C42#1-K1-C62-C102	-81.40(15)	C53-K2-C13-C63	-30.81(12)
C42-K1-C62-C102	-146.77(17)	C63#1-K2-C13-C63	-118.2(2)
C32#1-K1-C62-C102	-53.43(15)	C43#1-K2-C13-C63	-29.92(16)
C32-K1-C62-C102	-179.11(16)	C43-K2-C13-C63	-63.33(13)
C22#1-K1-C62-C102	-31.73(17)	C13#1-K2-C13-C63	131.96(12)
C32-C22-C72-C92	61.2(3)	C33#1-K2-C13-C63	9.25(17)
C12-C22-C72-C92	-120.8(3)	C33-K2-C13-C63	-95.60(14)
K1-C22-C72-C92	-30.5(3)	C23#1-K2-C13-C63	52.41(18)
C32-C22-C72-C82	-63.0(3)	S1-K2-C13-N21	15.76(14)
C12-C22-C72-C82	115.0(2)	C53#1-K2-C13-N21	174.30(13)
K1-C22-C72-C82	-154.70(17)	C53-K2-C13-N21	-147.01(18)
C52-C62-C102-C122	40.6(3)	C63-K2-C13-N21	-116.2(2)
C12-C62-C102-C122	-142.2(2)	C63#1-K2-C13-N21	125.60(17)
K1-C62-C102-C122	128.14(16)	C43#1-K2-C13-N21	-146.12(14)
C52-C62-C102-C112	-83.9(2)	C43-K2-C13-N21	-179.53(17)
C12-C62-C102-C112	93.3(2)	C13#1-K2-C13-N21	15.76(14)
K1-C62-C102-C112	3.7(2)	C33#1-K2-C13-N21	-106.95(15)
C41-N21-C13-C23	-102.1(2)	C33-K2-C13-N21	148.19(18)
Fe1-N21-C13-C23	81.8(2)	C23#1-K2-C13-N21	-63.8(2)
C41-N21-C13-C63	80.4(3)	C63-C13-C23-C33	2.1(3)
Fe1-N21-C13-C63	-95.71(19)	N21-C13-C23-C33	-175.37(17)

K2-C13-C23-C33	-64.06(17)	C13#1-K2-C23-C73	36.0(2)
C63-C13-C23-C73	-177.52(18)	C33#1-K2-C23-C73	158.69(15)
N21-C13-C23-C73	5.0(3)	C33-K2-C23-C73	116.1(2)
K2-C13-C23-C73	116.33(18)	C23#1-K2-C23-C73	137.78(15)
C63-C13-C23-K2	66.15(17)	C13-C23-C33-C43	-1.5(3)
N21-C13-C23-K2	-111.31(16)	C73-C23-C33-C43	178.15(19)
S1-K2-C23-C33	-158.34(13)	K2-C23-C33-C43	-64.93(19)
C53#1-K2-C23-C33	-17.77(16)	C13-C23-C33-K2	63.45(17)
C53-K2-C23-C33	61.56(14)	C73-C23-C33-K2	-116.92(17)
C63-K2-C23-C33	95.28(15)	S1-K2-C33-C43	151.02(11)
C63#1-K2-C23-C33	-51.03(16)	C53#1-K2-C33-C43	-67.51(14)
C43#1-K2-C23-C33	14.56(17)	C53-K2-C33-C43	30.22(12)
C43-K2-C23-C33	28.88(13)	C63-K2-C33-C43	63.79(13)
C13-K2-C23-C33	125.52(19)	C63#1-K2-C33-C43	-91.34(14)
C13#1-K2-C23-C33	-80.16(18)	C43#1-K2-C33-C43	-41.77(17)
C33#1-K2-C23-C33	42.6(2)	C13-K2-C33-C43	97.24(15)
C23#1-K2-C23-C33	21.67(13)	C13#1-K2-C33-C43	-95.87(15)
S1-K2-C23-C13	76.14(11)	C33#1-K2-C33-C43	-28.97(11)
C53#1-K2-C23-C13	-143.29(11)	C23#1-K2-C33-C43	-52.1(2)
C53-K2-C23-C13	-63.96(12)	S1-K2-C33-C23	23.92(14)
C63-K2-C23-C13	-30.24(11)	C53#1-K2-C33-C23	165.38(13)
C63#1-K2-C23-C13	-176.55(11)	C53-K2-C33-C23	-96.89(15)
C43#1-K2-C23-C13	-110.96(12)	C63-K2-C33-C23	-63.32(13)
C43-K2-C23-C13	-96.64(14)	C63#1-K2-C33-C23	141.55(13)
C13#1-K2-C23-C13	154.32(17)	C43#1-K2-C33-C23	-168.88(13)
C33#1-K2-C23-C13	-82.95(17)	C43-K2-C33-C23	-127.1(2)
C33-K2-C23-C13	-125.52(19)	C13-K2-C33-C23	-29.87(12)
C23#1-K2-C23-C13	-103.85(11)	C13#1-K2-C33-C23	137.02(12)
S1-K2-C23-C73	-42.23(15)	C33#1-K2-C33-C23	-156.08(14)
C53#1-K2-C23-C73	98.34(16)	C23#1-K2-C33-C23	-179.17(6)
C53-K2-C23-C73	177.67(18)	C23-C33-C43-C53	-0.1(3)
C63-K2-C23-C73	-148.61(18)	K2-C33-C43-C53	-66.33(19)
C63#1-K2-C23-C73	65.08(17)	C23-C33-C43-K2	66.26(19)
C43#1-K2-C23-C73	130.67(15)	S1-K2-C43-C53	85.40(15)
C43-K2-C23-C73	144.99(19)	C53#1-K2-C43-C53	-120.41(13)
C13-K2-C23-C73	-118.4(2)	C63-K2-C43-C53	29.87(12)

C63#1-K2-C43-C53	-135.01(13)	C13#1-K2-C53-C63	-143.74(13)
C43#1-K2-C43-C53	-94.60(15)	C33#1-K2-C53-C63	-125.01(14)
C13-K2-C43-C53	63.21(13)	C33-K2-C53-C63	96.17(15)
C13#1-K2-C43-C53	-121.06(13)	C23#1-K2-C53-C63	-117.22(14)
C33#1-K2-C43-C53	-77.74(14)	C43-C53-C63-C13	-0.4(3)
C33-K2-C43-C53	124.79(19)	K2-C53-C63-C13	-67.77(17)
C23#1-K2-C43-C53	-84.36(14)	C43-C53-C63-C103	177.0(2)
S1-K2-C43-C33	-39.39(15)	K2-C53-C63-C103	109.62(19)
C53#1-K2-C43-C33	114.80(13)	C43-C53-C63-K2	67.38(19)
C53-K2-C43-C33	-124.79(19)	C23-C13-C63-C53	-1.2(3)
C63-K2-C43-C33	-94.92(14)	N21-C13-C63-C53	176.29(18)
C63#1-K2-C43-C33	100.20(13)	K2-C13-C63-C53	66.91(18)
C43#1-K2-C43-C33	140.61(16)	C23-C13-C63-C103	-178.54(19)
C13-K2-C43-C33	-61.58(12)	N21-C13-C63-C103	-1.1(3)
C13#1-K2-C43-C33	114.15(13)	K2-C13-C63-C103	-110.4(2)
C33#1-K2-C43-C33	157.47(10)	C23-C13-C63-K2	-68.11(17)
C23#1-K2-C43-C33	150.85(12)	N21-C13-C63-K2	109.38(16)
C33-C43-C53-C63	1.0(3)	S1-K2-C63-C53	-173.18(13)
K2-C43-C53-C63	-66.74(19)	C53#1-K2-C63-C53	10.8(2)
C33-C43-C53-K2	67.76(19)	C63#1-K2-C63-C53	6.82(13)
S1-K2-C53-C43	-117.73(12)	C43#1-K2-C63-C53	34.26(16)
C53#1-K2-C53-C43	62.27(12)	C43-K2-C63-C53	-29.05(13)
C63-K2-C53-C43	-126.3(2)	C13-K2-C63-C53	-124.0(2)
C63#1-K2-C53-C43	57.34(16)	C13#1-K2-C63-C53	80.1(2)
C43#1-K2-C53-C43	85.01(16)	C33#1-K2-C63-C53	62.41(15)
C13-K2-C53-C43	-95.60(15)	C33-K2-C63-C53	-61.63(14)
C13#1-K2-C53-C43	89.99(17)	C23#1-K2-C63-C53	84.36(16)
C33#1-K2-C53-C43	108.72(14)	S1-K2-C63-C13	-49.20(12)
C33-K2-C53-C43	-30.10(12)	C53#1-K2-C63-C13	134.74(12)
C23#1-K2-C53-C43	116.51(14)	C53-K2-C63-C13	124.0(2)
S1-K2-C53-C63	8.53(16)	C63#1-K2-C63-C13	130.80(12)
C53#1-K2-C53-C63	-171.47(16)	C43#1-K2-C63-C13	158.24(12)
C63#1-K2-C53-C63	-176.39(7)	C43-K2-C63-C13	94.93(15)
C43#1-K2-C53-C63	-148.72(15)	C13#1-K2-C63-C13	-155.95(17)
C43-K2-C53-C63	126.3(2)	C33#1-K2-C63-C13	-173.61(12)
C13-K2-C53-C63	30.67(13)	C33-K2-C63-C13	62.35(13)

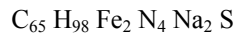
C23#1-K2-C63-C13	-151.66(12)	C33-C23-C73-C83	-57.3(3)
S1-K2-C63-C103	70.05(14)	C13-C23-C73-C83	122.3(2)
C53#1-K2-C63-C103	-106.01(15)	K2-C23-C73-C83	-147.54(15)
C53-K2-C63-C103	-116.8(2)	C33-C23-C73-C93	65.7(3)
C63#1-K2-C63-C103	-109.95(14)	C13-C23-C73-C93	-114.7(2)
C43#1-K2-C63-C103	-82.51(15)	K2-C23-C73-C93	-24.5(2)
C43-K2-C63-C103	-145.82(17)	C53-C63-C103-C123	-75.7(3)
C13-K2-C63-C103	119.3(2)	C13-C63-C103-C123	101.6(2)
C13#1-K2-C63-C103	-36.7(2)	K2-C63-C103-C123	11.6(2)
C33#1-K2-C63-C103	-54.36(15)	C53-C63-C103-C113	48.6(3)
C33-K2-C63-C103	-178.40(16)	C13-C63-C103-C113	-134.1(2)
C23#1-K2-C63-C103	-32.41(17)	K2-C63-C103-C113	135.94(18)

Symmetry transformations used to generate equivalent atoms:

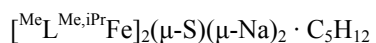
#1 -x+1,y,-z+3/2

REFERENCE NUMBER: holmr37

CRYSTAL STRUCTURE REPORT



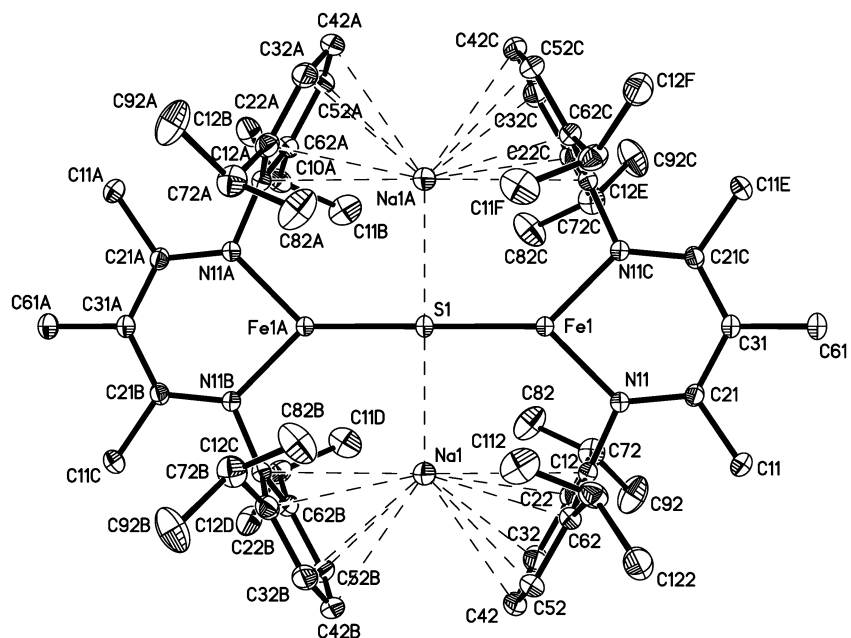
or



Report prepared for:

M. Rodriguez, Prof. P. Holland

December 15, 2011



William W. Brennessel

X-ray Crystallographic Facility

Department of Chemistry, University of Rochester

120 Trustee Road

Rochester, NY 14627

Data collection

A crystal ($0.36 \times 0.20 \times 0.16 \text{ mm}^3$) was placed onto the tip of a 0.1 mm diameter glass capillary tube or fiber and mounted on a Bruker SMART APEX II CCD Platform diffractometer for a data collection at $100.0(5) \text{ K}$.¹ A preliminary set of cell constants and an orientation matrix were calculated from reflections harvested from three orthogonal wedges of reciprocal space. The full data collection was carried out using MoK α radiation (graphite monochromator) with a frame time of 25 seconds and a detector distance of 4.01 cm. A randomly oriented region of reciprocal space was surveyed: six major sections of frames were collected with 0.50° steps in ω at six different ϕ settings and a detector position of -38° in 2θ . The intensity data were corrected for absorption.² Final cell constants were calculated from the xyz centroids of 3993 strong reflections from the actual data collection after integration.³ See Table 1 for additional crystal and refinement information.

Structure solution and refinement

The structure was solved using SIR97⁴ and refined using SHELXL-97.⁵ The space group $I2/m$ was determined based on systematic absences and intensity statistics. A direct-methods solution was calculated which provided most non-hydrogen atoms from the E-map. Full-matrix least squares / difference Fourier cycles were performed which located the remaining non-hydrogen atoms. All non-hydrogen atoms were refined with anisotropic displacement parameters. All hydrogen atoms were placed in ideal positions and refined as riding atoms with relative isotropic displacement parameters. The final full matrix least squares refinement converged to $R1 = 0.0399$ ($F^2, I > 2\sigma(I)$) and $wR2 = 0.1075$ ($F^2, \text{all data}$).

Structure description

The structure is the one suggested. The di-iron and co-crystallized pentane solvent molecules both lie in crystallographic 2/m positions; thus one-fourth of each is unique. The pentane molecule is modeled as disordered over the 2/m position (25:25:25:25).

Unless noted otherwise all structural diagrams containing thermal displacement ellipsoids are drawn at the 50 % probability level.

Data collection, structure solution, and structure refinement were conducted at the X-ray Crystallographic Facility, B51 Hutchison Hall, Department of Chemistry, University of Rochester. All publications arising from this report MUST either 1) include William W. Brennessel as a coauthor or 2) acknowledge William W. Brennessel and the X-ray Crystallographic Facility of the Department of Chemistry at the University of Rochester.

¹ APEX2, version 2011.4-1; Bruker AXS: Madison, WI, 2011.

² Sheldrick, G. M. SADABS, version 2008/1; University of Göttingen: Göttingen, Germany, 2008.

³ SAINT, version 7.68A; Bruker AXS: Madison, WI, 2009.

⁴ Altomare, A.; Burla, M. C.; Camalli, M.; Cascarano, G. L.; Giacovazzo, C.; Guagliardi, A.; Moliterni, A. G. G.; Polidori, G.; Spagna, R. SIR97: A new program for solving and refining crystal structures; Istituto di Cristallografia, CNR: Bari, Italy, 1999.

⁵ Sheldrick, G. M. *Acta Cryst.* **2008**, *A64*, 112-122.

Some equations of interest:

$$R_{\text{int}} = \sum |F_o^2 - \langle F_o^2 \rangle| / \sum |F_o^2|$$

$$R1 = \sum \|F_o\| - \|F_c\| / \sum |F_o|$$

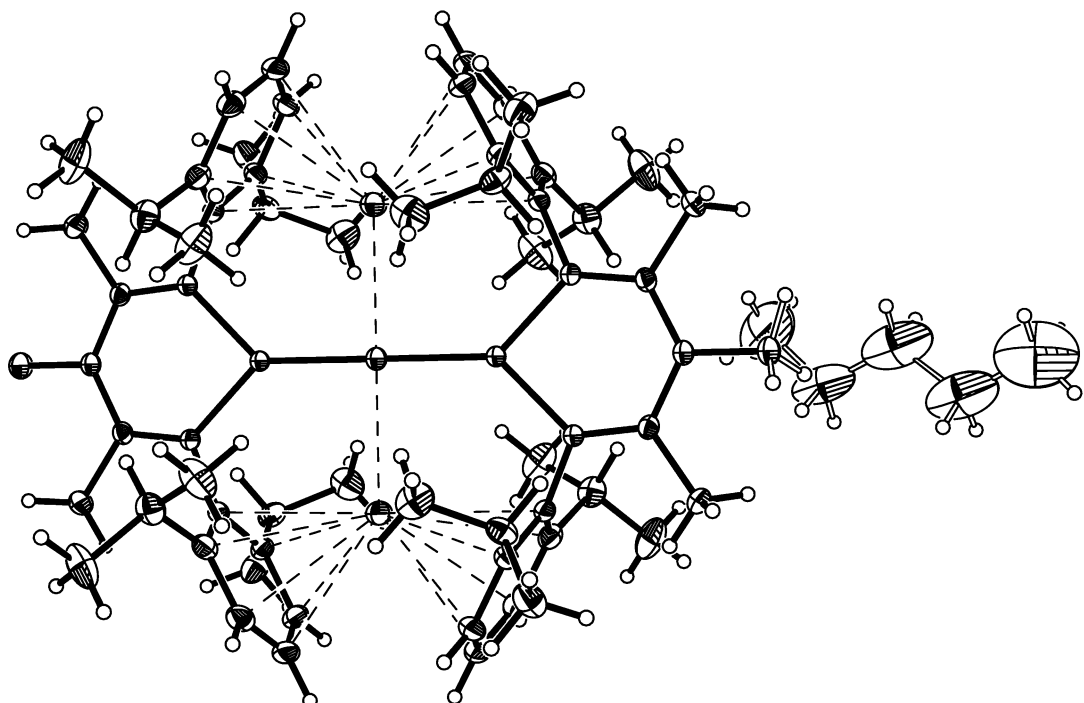
$$wR2 = [\sum [w(F_o^2 - F_c^2)^2] / \sum [w(F_o^2)^2]]^{1/2}$$

where $w = 1 / [\sigma^2(F_o^2) + (aP)^2 + bP]$ and

$$P = 1/3 \max(0, F_o^2) + 2/3 F_c^2$$

$$\text{GOF} = S = [\sum [w(F_o^2 - F_c^2)^2] / (m-n)]^{1/2}$$

where m = number of reflections and n = number of parameters



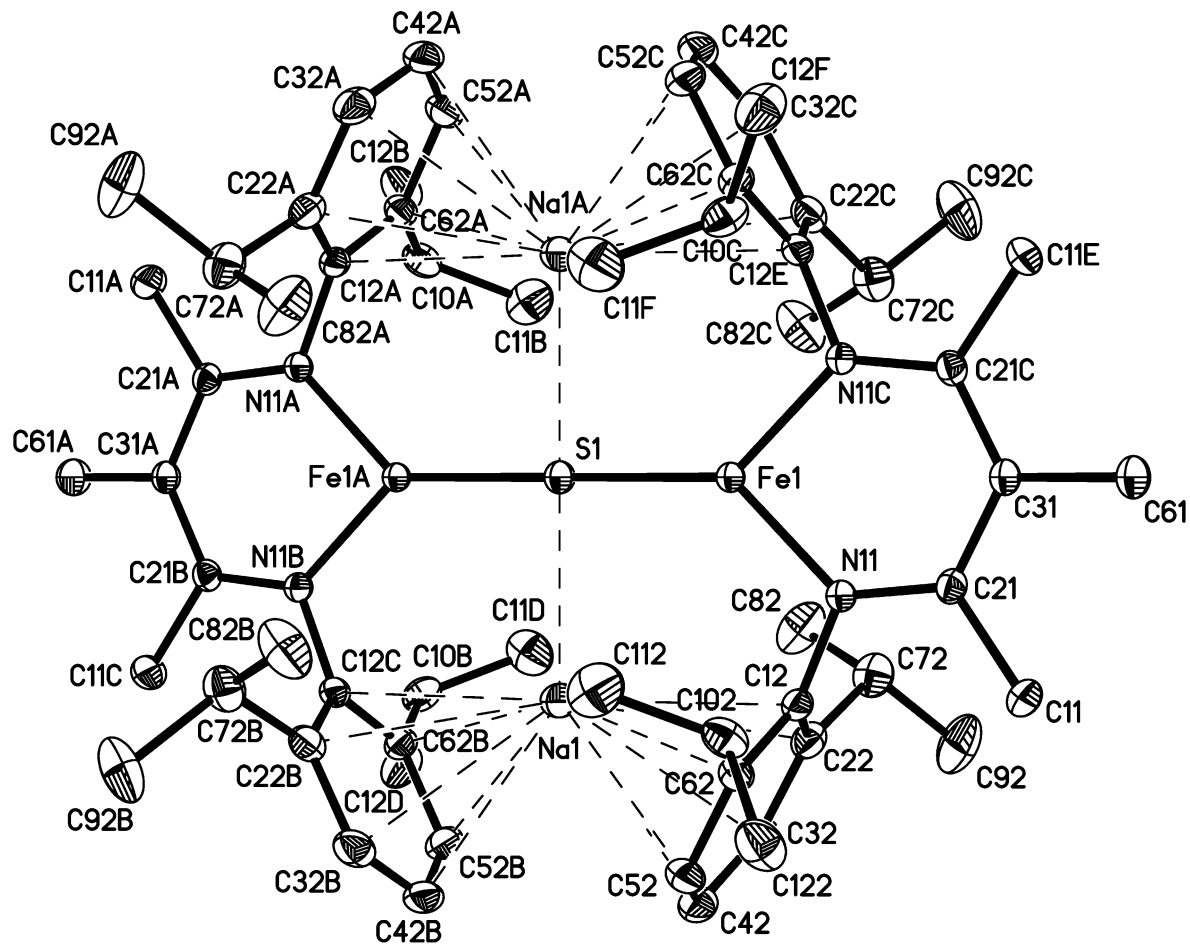


Table 1. Crystal data and structure refinement for holmr37.

Identification code	holmr37		
Empirical formula	C65 H98 Fe2 N4 Na2 S		
Formula weight	1125.21		
Temperature	100.0(5) K		
Wavelength	0.71073 Å		
Crystal system	Monoclinic		
Space group	<i>I</i> 2/m		
Unit cell dimensions	<i>a</i> = 12.007(3) Å	α = 90°	
	<i>b</i> = 19.936(3) Å	β = 97.963(2)°	
	<i>c</i> = 13.4470(17) Å	γ = 90°	
Volume	3187.8(9) Å ³		
<i>Z</i>	2		
Density (calculated)	1.172 Mg/m ³		
Absorption coefficient	0.542 mm ⁻¹		
<i>F</i> (000)	1212		
Crystal color, morphology	green-black, block		
Crystal size	0.36 x 0.20 x 0.16 mm ³		
Theta range for data collection	1.84 to 37.78°		
Index ranges	-20 ≤ <i>h</i> ≤ 20, -34 ≤ <i>k</i> ≤ 34, -23 ≤ <i>l</i> ≤ 23		
Reflections collected	58864		
Independent reflections	8744 [<i>R</i> (int) = 0.0570]		
Observed reflections	6726		
Completeness to theta = 37.78°	99.9%		
Absorption correction	Multi-scan		
Max. and min. transmission	0.9184 and 0.8289		
Refinement method	Full-matrix least-squares on <i>F</i> ²		
Data / restraints / parameters	8744 / 8 / 210		
Goodness-of-fit on <i>F</i> ²	1.071		
Final <i>R</i> indices [<i>I</i> >2sigma(<i>I</i>)]	<i>R</i> 1 = 0.0399, <i>wR</i> 2 = 0.0978		
<i>R</i> indices (all data)	<i>R</i> 1 = 0.0586, <i>wR</i> 2 = 0.1075		
Largest diff. peak and hole	0.739 and -0.304 e.Å ⁻³		

Table 2. Atomic coordinates ($x \times 10^4$) and equivalent isotropic displacement parameters ($\text{\AA}^2 \times 10^3$) for holmr37. U_{eq} is defined as one third of the trace of the orthogonalized U_{ij} tensor.

	x	y	z	U_{eq}
Fe1	9416(1)	0	1477(1)	14(1)
S1	10000	0	0	20(1)
Na1	10000	1354(1)	0	25(1)
N11	9042(1)	693(1)	2387(1)	15(1)
C11	8490(1)	1257(1)	3872(1)	25(1)
C21	8734(1)	627(1)	3311(1)	16(1)
C31	8622(1)	0	3771(1)	16(1)
C61	8382(1)	0	4854(1)	24(1)
C12	9102(1)	1341(1)	1962(1)	16(1)
C22	8159(1)	1605(1)	1341(1)	21(1)
C32	8272(1)	2217(1)	857(1)	26(1)
C42	9275(1)	2570(1)	990(1)	27(1)
C52	10192(1)	2315(1)	1622(1)	24(1)
C62	10122(1)	1705(1)	2122(1)	19(1)
C72	7042(1)	1241(1)	1205(1)	26(1)
C82	6752(1)	974(1)	133(1)	39(1)
C92	6094(1)	1693(1)	1473(1)	42(1)
C102	11120(1)	1437(1)	2826(1)	23(1)
C112	12030(1)	1167(1)	2241(1)	36(1)
C122	11607(1)	1964(1)	3590(1)	31(1)
C14	5266(12)	-195(11)	2832(12)	126(9)
C24	5259(8)	302(6)	3677(12)	81(6)
C34	5005(9)	-36(9)	4640(10)	107(4)
C44	4950(9)	415(6)	5543(10)	107(4)
C54	4806(14)	70(20)	6523(19)	143(10)

Table 3. Bond lengths [\AA] and angles [$^\circ$] for holmr37.

Fe(1)-N(11)#1	1.9387(7)	C(22)-C(72)	1.5143(15)
Fe(1)-N(11)	1.9388(7)	C(32)-C(42)	1.3839(17)
Fe(1)-S(1)	2.1957(3)	C(32)-H(32A)	0.9500
Fe(1)-Na(1)#2	3.4796(6)	C(42)-C(52)	1.3903(16)
Fe(1)-Na(1)	3.4796(6)	C(42)-H(42A)	0.9500
S(1)-Fe(1)#2	2.1957(3)	C(52)-C(62)	1.3984(13)
S(1)-Na(1)#2	2.6994(7)	C(52)-H(52A)	0.9500
S(1)-Na(1)	2.6994(7)	C(62)-C(102)	1.5163(14)
Na(1)-C(52)#3	2.8884(11)	C(72)-C(82)	1.5318(16)
Na(1)-C(52)	2.8884(11)	C(72)-C(92)	1.5333(16)
Na(1)-C(62)#3	2.9218(10)	C(72)-H(72A)	1.0000
Na(1)-C(62)	2.9218(10)	C(82)-H(82A)	0.9800
Na(1)-C(42)	2.9537(12)	C(82)-H(82B)	0.9800
Na(1)-C(42)#3	2.9537(12)	C(82)-H(82C)	0.9800
Na(1)-C(12)	2.9845(9)	C(92)-H(92A)	0.9800
Na(1)-C(12)#3	2.9845(9)	C(92)-H(92B)	0.9800
Na(1)-C(32)	3.0421(11)	C(92)-H(92C)	0.9800
Na(1)-C(32)#3	3.0422(11)	C(102)-C(122)	1.5280(15)
Na(1)-C(22)#3	3.0804(10)	C(102)-C(112)	1.5297(17)
N(11)-C(21)	1.3517(11)	C(102)-H(10A)	1.0000
N(11)-C(12)	1.4193(11)	C(112)-H(11D)	0.9800
C(11)-C(21)	1.5150(13)	C(112)-H(11E)	0.9800
C(11)-H(11A)	0.9800	C(112)-H(11F)	0.9800
C(11)-H(11B)	0.9800	C(122)-H(12A)	0.9800
C(11)-H(11C)	0.9800	C(122)-H(12B)	0.9800
C(21)-C(31)	1.4087(10)	C(122)-H(12C)	0.9800
C(31)-C(21)#1	1.4088(10)	C(14)-C(24)	1.509(8)
C(31)-C(61)	1.5229(18)	C(14)-H(14A)	0.9800
C(61)-H(61A)	0.9800	C(14)-H(14B)	0.9800
C(61)-H(61B)	0.9800	C(14)-H(14C)	0.9800
C(61)-H(61C)	0.9800	C(24)-C(34)	1.528(9)
C(12)-C(22)	1.4122(13)	C(24)-H(24A)	0.9900
C(12)-C(62)	1.4134(13)	C(24)-H(24B)	0.9900
C(22)-C(32)	1.3978(14)	C(34)-C(44)	1.519(8)

C(34)-H(34A)	0.9900	C(52)-Na(1)-C(42)	27.51(3)
C(34)-H(34B)	0.9900	C(62)#3-Na(1)-C(42)	105.41(3)
C(44)-C(54)	1.517(7)	C(62)-Na(1)-C(42)	48.83(3)
C(44)-H(44A)	0.9900	S(1)-Na(1)-C(42)#3	145.14(2)
C(44)-H(44B)	0.9900	C(52)#3-Na(1)-C(42)#3	27.51(3)
C(54)-H(54A)	0.9800	C(52)-Na(1)-C(42)#3	78.37(3)
C(54)-H(54B)	0.9800	C(62)#3-Na(1)-C(42)#3	48.83(3)
C(54)-H(54C)	0.9800	C(62)-Na(1)-C(42)#3	105.41(3)
N(11)#1-Fe(1)-N(11)	90.88(4)	C(42)-Na(1)-C(42)#3	69.73(4)
N(11)#1-Fe(1)-S(1)	134.56(2)	S(1)-Na(1)-C(12)	89.51(2)
N(11)-Fe(1)-S(1)	134.56(2)	C(52)#3-Na(1)-C(12)	132.25(3)
N(11)#1-Fe(1)-Na(1)#2	83.69(2)	C(52)-Na(1)-C(12)	48.62(3)
N(11)-Fe(1)-Na(1)#2	174.54(2)	C(62)#3-Na(1)-C(12)	152.84(3)
S(1)-Fe(1)-Na(1)#2	50.875(8)	C(62)-Na(1)-C(12)	27.67(3)
N(11)#1-Fe(1)-Na(1)	174.54(2)	C(42)-Na(1)-C(12)	56.20(3)
N(11)-Fe(1)-Na(1)	83.68(2)	C(42)#3-Na(1)-C(12)	124.77(3)
S(1)-Fe(1)-Na(1)	50.876(8)	S(1)-Na(1)-C(12)#3	89.51(2)
Na(1)#2-Fe(1)-Na(1)	101.751(16)	C(52)#3-Na(1)-C(12)#3	48.62(3)
Fe(1)#2-S(1)-Fe(1)	180.0	C(52)-Na(1)-C(12)#3	132.25(3)
Fe(1)#2-S(1)-Na(1)#2	90.0	C(62)#3-Na(1)-C(12)#3	27.67(3)
Fe(1)-S(1)-Na(1)#2	90.0	C(62)-Na(1)-C(12)#3	152.84(3)
Fe(1)#2-S(1)-Na(1)	90.0	C(42)-Na(1)-C(12)#3	124.77(3)
Fe(1)-S(1)-Na(1)	90.0	C(42)#3-Na(1)-C(12)#3	56.20(3)
Na(1)#2-S(1)-Na(1)	180.0	C(12)-Na(1)-C(12)#3	179.02(4)
S(1)-Na(1)-C(52)#3	131.56(2)	S(1)-Na(1)-C(32)	124.45(2)
S(1)-Na(1)-C(52)	131.55(2)	C(52)#3-Na(1)-C(32)	85.62(3)
C(52)#3-Na(1)-C(52)	96.89(4)	C(52)-Na(1)-C(32)	47.62(3)
S(1)-Na(1)-C(62)#3	103.84(2)	C(62)#3-Na(1)-C(32)	106.85(3)
C(52)#3-Na(1)-C(62)#3	27.85(3)	C(62)-Na(1)-C(32)	55.91(3)
C(52)-Na(1)-C(62)#3	124.53(3)	C(42)-Na(1)-C(32)	26.64(3)
S(1)-Na(1)-C(62)	103.84(2)	C(42)#3-Na(1)-C(32)	88.03(4)
C(52)#3-Na(1)-C(62)	124.53(3)	C(12)-Na(1)-C(32)	47.27(3)
C(52)-Na(1)-C(62)	27.85(3)	C(12)#3-Na(1)-C(32)	133.49(3)
C(62)#3-Na(1)-C(62)	152.32(4)	S(1)-Na(1)-C(32)#3	124.45(2)
S(1)-Na(1)-C(42)	145.14(2)	C(52)#3-Na(1)-C(32)#3	47.62(3)
C(52)#3-Na(1)-C(42)	78.37(3)	C(52)-Na(1)-C(32)#3	85.62(3)

C(62)#3-Na(1)-C(32)#3	55.91(3)	C(22)-C(12)-C(62)	120.40(8)
C(62)-Na(1)-C(32)#3	106.85(3)	C(22)-C(12)-N(11)	119.76(8)
C(42)-Na(1)-C(32)#3	88.03(4)	C(62)-C(12)-N(11)	119.78(8)
C(42)#3-Na(1)-C(32)#3	26.64(3)	C(22)-C(12)-Na(1)	80.36(5)
C(12)-Na(1)-C(32)#3	133.49(3)	C(62)-C(12)-Na(1)	73.70(5)
C(12)#3-Na(1)-C(32)#3	47.27(3)	N(11)-C(12)-Na(1)	114.11(5)
C(32)-Na(1)-C(32)#3	111.10(5)	C(32)-C(22)-C(12)	118.62(9)
S(1)-Na(1)-C(22)#3	99.36(2)	C(32)-C(22)-C(72)	120.27(9)
C(52)#3-Na(1)-C(22)#3	55.85(3)	C(12)-C(22)-C(72)	121.11(9)
C(52)-Na(1)-C(22)#3	110.21(3)	C(32)-C(22)-Na(1)	75.28(6)
C(62)#3-Na(1)-C(22)#3	48.13(3)	C(12)-C(22)-Na(1)	72.77(5)
C(62)-Na(1)-C(22)#3	126.13(3)	C(72)-C(22)-Na(1)	123.16(6)
C(42)-Na(1)-C(22)#3	114.23(3)	C(42)-C(32)-C(22)	121.44(9)
C(42)#3-Na(1)-C(22)#3	47.36(3)	C(42)-C(32)-Na(1)	73.12(6)
C(12)-Na(1)-C(22)#3	153.48(3)	C(22)-C(32)-Na(1)	78.34(6)
C(12)#3-Na(1)-C(22)#3	26.87(2)	C(42)-C(32)-H(32A)	119.3
C(32)-Na(1)-C(22)#3	135.38(4)	C(22)-C(32)-H(32A)	119.3
C(32)#3-Na(1)-C(22)#3	26.38(3)	Na(1)-C(32)-H(32A)	120.2
C(21)-N(11)-C(12)	119.68(7)	C(32)-C(42)-C(52)	119.63(9)
C(21)-N(11)-Fe(1)	128.87(6)	C(32)-C(42)-Na(1)	80.25(6)
C(12)-N(11)-Fe(1)	111.44(5)	C(52)-C(42)-Na(1)	73.63(6)
C(21)-C(11)-H(11A)	109.5	C(32)-C(42)-H(42A)	120.2
C(21)-C(11)-H(11B)	109.5	C(52)-C(42)-H(42A)	120.2
H(11A)-C(11)-H(11B)	109.5	Na(1)-C(42)-H(42A)	116.7
C(21)-C(11)-H(11C)	109.5	C(42)-C(52)-C(62)	121.13(10)
H(11A)-C(11)-H(11C)	109.5	C(42)-C(52)-Na(1)	78.86(6)
H(11B)-C(11)-H(11C)	109.5	C(62)-C(52)-Na(1)	77.41(6)
N(11)-C(21)-C(31)	123.06(8)	C(42)-C(52)-H(52A)	119.4
N(11)-C(21)-C(11)	118.23(8)	C(62)-C(52)-H(52A)	119.4
C(31)-C(21)-C(11)	118.71(8)	Na(1)-C(52)-H(52A)	114.7
C(21)-C(31)-C(21)#1	124.94(11)	C(52)-C(62)-C(12)	118.72(9)
C(21)-C(31)-C(61)	117.53(5)	C(52)-C(62)-C(102)	120.76(9)
C(21)#1-C(31)-C(61)	117.53(5)	C(12)-C(62)-C(102)	120.52(8)
C(31)-C(61)-H(61A)	109.5	C(52)-C(62)-Na(1)	74.75(6)
C(31)-C(61)-H(61B)	109.5	C(12)-C(62)-Na(1)	78.63(5)
C(31)-C(61)-H(61C)	109.5	C(102)-C(62)-Na(1)	116.98(6)

C(22)-C(72)-C(82)	111.24(9)	C(102)-C(112)-H(11F)	109.5
C(22)-C(72)-C(92)	111.33(10)	H(11D)-C(112)-H(11F)	109.5
C(82)-C(72)-C(92)	110.24(9)	H(11E)-C(112)-H(11F)	109.5
C(22)-C(72)-H(72A)	108.0	C(102)-C(122)-H(12A)	109.5
C(82)-C(72)-H(72A)	108.0	C(102)-C(122)-H(12B)	109.5
C(92)-C(72)-H(72A)	108.0	H(12A)-C(122)-H(12B)	109.5
C(72)-C(82)-H(82A)	109.5	C(102)-C(122)-H(12C)	109.5
C(72)-C(82)-H(82B)	109.5	H(12A)-C(122)-H(12C)	109.5
H(82A)-C(82)-H(82B)	109.5	H(12B)-C(122)-H(12C)	109.5
C(72)-C(82)-H(82C)	109.5	C(14)-C(24)-C(34)	111.8(10)
H(82A)-C(82)-H(82C)	109.5	C(14)-C(24)-H(24A)	109.3
H(82B)-C(82)-H(82C)	109.5	C(34)-C(24)-H(24A)	109.3
C(72)-C(92)-H(92A)	109.5	C(14)-C(24)-H(24B)	109.3
C(72)-C(92)-H(92B)	109.5	C(34)-C(24)-H(24B)	109.3
H(92A)-C(92)-H(92B)	109.5	H(24A)-C(24)-H(24B)	107.9
C(72)-C(92)-H(92C)	109.5	C(44)-C(34)-C(24)	116.9(13)
H(92A)-C(92)-H(92C)	109.5	C(44)-C(34)-H(34A)	108.1
H(92B)-C(92)-H(92C)	109.5	C(24)-C(34)-H(34A)	108.1
C(62)-C(102)-C(122)	111.94(9)	C(44)-C(34)-H(34B)	108.1
C(62)-C(102)-C(112)	111.20(9)	C(24)-C(34)-H(34B)	108.1
C(122)-C(102)-C(112)	110.73(9)	H(34A)-C(34)-H(34B)	107.3
C(62)-C(102)-H(10A)	107.6	C(54)-C(44)-C(34)	116.8(18)
C(122)-C(102)-H(10A)	107.6	C(54)-C(44)-H(44A)	108.1
C(112)-C(102)-H(10A)	107.6	C(34)-C(44)-H(44A)	108.1
C(102)-C(112)-H(11D)	109.5	C(54)-C(44)-H(44B)	108.1
C(102)-C(112)-H(11E)	109.5	C(34)-C(44)-H(44B)	108.1
H(11D)-C(112)-H(11E)	109.5	H(44A)-C(44)-H(44B)	107.3

Symmetry transformations used to generate equivalent atoms:

#1 x,-y,z #2 -x+2,-y,-z #3 -x+2,y,-z

Table 4. Anisotropic displacement parameters ($\text{\AA}^2 \times 10^3$) for holmr37. The anisotropic displacement factor exponent takes the form: $-2\pi^2 [h^2 a^{*2} U_{11} + \dots + 2 h k a^{*} b^{*} U_{12}]$

	U_{11}	U_{22}	U_{33}	U_{23}	U_{13}	U_{12}
Fe1	17(1)	13(1)	12(1)	0	5(1)	0
S1	30(1)	16(1)	15(1)	0	10(1)	0
Na1	39(1)	18(1)	20(1)	0	10(1)	0
N11	18(1)	14(1)	13(1)	0(1)	4(1)	0(1)
C11	37(1)	19(1)	21(1)	-4(1)	13(1)	0(1)
C21	17(1)	17(1)	14(1)	-2(1)	4(1)	0(1)
C31	18(1)	17(1)	13(1)	0	4(1)	0
C61	35(1)	24(1)	16(1)	0	10(1)	0
C12	21(1)	14(1)	14(1)	0(1)	5(1)	1(1)
C22	24(1)	20(1)	18(1)	0(1)	4(1)	6(1)
C32	36(1)	23(1)	20(1)	5(1)	6(1)	11(1)
C42	45(1)	17(1)	23(1)	5(1)	13(1)	6(1)
C52	35(1)	17(1)	23(1)	2(1)	10(1)	-4(1)
C62	24(1)	16(1)	17(1)	0(1)	5(1)	-2(1)
C72	20(1)	31(1)	27(1)	1(1)	1(1)	6(1)
C82	28(1)	47(1)	41(1)	-17(1)	1(1)	5(1)
C92	26(1)	59(1)	42(1)	-15(1)	7(1)	8(1)
C102	23(1)	22(1)	24(1)	2(1)	0(1)	-6(1)
C112	24(1)	38(1)	44(1)	-8(1)	0(1)	1(1)
C122	35(1)	34(1)	22(1)	-2(1)	2(1)	-14(1)
C14	84(8)	112(16)	197(18)	-65(15)	73(11)	-46(9)
C24	22(4)	52(6)	164(17)	-32(8)	1(6)	0(4)
C34	34(2)	74(5)	213(12)	-46(8)	13(6)	-15(5)
C44	34(2)	74(5)	213(12)	-46(8)	13(6)	-15(5)
C54	82(12)	140(30)	190(20)	20(40)	-40(16)	40(20)

Table 5. Hydrogen coordinates ($x \times 10^4$) and isotropic displacement parameters ($\text{\AA}^2 \times 10^3$) for holmr37.

	x	y	z	U(eq)
H11A	8492	1645	3425	37
H11B	9070	1316	4454	37
H11C	7752	1217	4099	37
H61A	8390	-462	5104	36
H61B	7642	200	4885	36
H61C	8960	262	5270	36
H32A	7647	2395	427	31
H42A	9336	2983	651	33
H52A	10877	2560	1716	29
H72A	7108	849	1673	31
H82A	7362	685	-29	59
H82B	6655	1351	-339	59
H82C	6053	715	79	59
H92A	6310	1884	2144	63
H92B	5405	1428	1465	63
H92C	5961	2057	980	63
H10A	10847	1054	3207	28
H11D	11711	813	1782	53
H11E	12651	984	2711	53
H11F	12309	1532	1854	53
H12A	11016	2123	3967	46
H12B	11899	2342	3239	46
H12C	12218	1764	4055	46
H14A	5923	-489	2974	189
H14B	5300	47	2202	189
H14C	4578	-466	2770	189
H24A	4686	651	3474	97
H24B	6002	525	3807	97
H34A	4276	-272	4488	129
H34B	5588	-381	4832	129

H44A	5648	684	5653	129
H44B	4316	731	5374	129
H54A	4070	-149	6457	215
H54B	4856	405	7062	215
H54C	5400	-265	6683	215

Table 6. Torsion angles [°] for holmr37.

N11#1-Fe1-S1-Fe1#2	-29(16)	Fe1#2-S1-Na1-C32	143.45(2)
N11-Fe1-S1-Fe1#2	153(16)	Fe1-S1-Na1-C32	-36.55(2)
Na1#2-Fe1-S1-Fe1#2	-28(16)	Na1#2-S1-Na1-C32	-152.94(2)
Na1-Fe1-S1-Fe1#2	152(16)	Fe1#2-S1-Na1-C32#3	-36.55(2)
N11#1-Fe1-S1-Na1#2	-0.65(3)	Fe1-S1-Na1-C32#3	143.45(2)
N11-Fe1-S1-Na1#2	-179.35(3)	Na1#2-S1-Na1-C32#3	27.06(2)
Na1-Fe1-S1-Na1#2	180.0	Fe1#2-S1-Na1-C22#3	-27.633(18)
N11#1-Fe1-S1-Na1	179.35(3)	Fe1-S1-Na1-C22#3	152.366(18)
N11-Fe1-S1-Na1	0.65(3)	Na1#2-S1-Na1-C22#3	35.976(19)
Na1#2-Fe1-S1-Na1	180.0	N11#1-Fe1-N11-C21	4.15(9)
Fe1#2-S1-Na1-C52#3	24.48(3)	S1-Fe1-N11-C21	-176.77(6)
Fe1-S1-Na1-C52#3	-155.52(3)	Na1#2-Fe1-N11-C21	8.5(3)
Na1#2-S1-Na1-C52#3	88.09(3)	Na1-Fe1-N11-C21	-176.27(8)
Fe1#2-S1-Na1-C52	-155.52(3)	N11#1-Fe1-N11-C12	-174.68(4)
Fe1-S1-Na1-C52	24.48(3)	S1-Fe1-N11-C12	4.40(8)
Na1#2-S1-Na1-C52	-91.91(3)	Na1#2-Fe1-N11-C12	-170.3(2)
Fe1#2-S1-Na1-C62#3	21.37(2)	Na1-Fe1-N11-C12	4.91(6)
Fe1-S1-Na1-C62#3	-158.63(2)	C12-N11-C21-C31	178.10(9)
Na1#2-S1-Na1-C62#3	84.98(2)	Fe1-N11-C21-C31	-0.64(13)
Fe1#2-S1-Na1-C62	-158.63(2)	C12-N11-C21-C11	-1.56(12)
Fe1-S1-Na1-C62	21.37(2)	Fe1-N11-C21-C11	179.70(7)
Na1#2-S1-Na1-C62	-95.02(2)	N11-C21-C31-C21#1	-4.92(19)
Fe1#2-S1-Na1-C42	167.72(4)	C11-C21-C31-C21#1	174.74(9)
Fe1-S1-Na1-C42	-12.29(4)	N11-C21-C31-C61	174.10(10)
Na1#2-S1-Na1-C42	-128.68(4)	C11-C21-C31-C61	-6.24(15)
Fe1#2-S1-Na1-C42#3	-12.28(4)	C21-N11-C12-C22	-92.63(10)
Fe1-S1-Na1-C42#3	167.71(4)	Fe1-N11-C12-C22	86.31(9)
Na1#2-S1-Na1-C42#3	51.33(4)	C21-N11-C12-C62	90.45(10)
Fe1#2-S1-Na1-C12	177.474(18)	Fe1-N11-C12-C62	-90.60(8)
Fe1-S1-Na1-C12	-2.527(18)	C21-N11-C12-Na1	174.82(6)
Na1#2-S1-Na1-C12	-118.917(18)	Fe1-N11-C12-Na1	-6.23(7)
Fe1#2-S1-Na1-C12#3	-2.526(18)	S1-Na1-C12-C22	-112.13(5)
Fe1-S1-Na1-C12#3	177.473(18)	C52#3-Na1-C12-C22	40.54(7)
Na1#2-S1-Na1-C12#3	61.083(18)	C52-Na1-C12-C22	94.79(6)

C62#3-Na1-C12-C22	8.36(10)	N11-C12-C22-Na1	-112.34(7)
C62-Na1-C12-C22	125.76(8)	S1-Na1-C22-C32	-163.28(6)
C42-Na1-C12-C22	61.17(6)	C52#3-Na1-C22-C32	-22.28(7)
C42#3-Na1-C12-C22	74.64(6)	C52-Na1-C22-C32	62.25(6)
C12#3-Na1-C12-C22	-112.15(5)	C62#3-Na1-C22-C32	-48.41(7)
C32-Na1-C12-C22	28.95(6)	C62-Na1-C22-C32	96.48(7)
C32#3-Na1-C12-C22	107.37(7)	C42-Na1-C22-C32	28.59(6)
C22#3-Na1-C12-C22	137.54(10)	C42#3-Na1-C22-C32	7.17(7)
S1-Na1-C12-C62	122.11(5)	C12-Na1-C22-C32	126.87(9)
C52#3-Na1-C12-C62	-85.22(6)	C12#3-Na1-C22-C32	-55.15(10)
C52-Na1-C12-C62	-30.97(5)	C32#3-Na1-C22-C32	27.21(9)
C62#3-Na1-C12-C62	-117.40(10)	C22#3-Na1-C22-C32	16.72(6)
C42-Na1-C12-C62	-64.59(6)	S1-Na1-C22-C12	69.85(5)
C42#3-Na1-C12-C62	-51.12(6)	C52#3-Na1-C22-C12	-149.15(6)
C12#3-Na1-C12-C62	122.08(5)	C52-Na1-C22-C12	-64.62(6)
C32-Na1-C12-C62	-96.81(6)	C62#3-Na1-C22-C12	-175.29(5)
C32#3-Na1-C12-C62	-18.40(7)	C62-Na1-C22-C12	-30.39(5)
C22#3-Na1-C12-C62	11.78(10)	C42-Na1-C22-C12	-98.28(6)
S1-Na1-C12-N11	6.26(6)	C42#3-Na1-C22-C12	-119.70(6)
C52#3-Na1-C12-N11	158.93(6)	C12#3-Na1-C22-C12	177.97(8)
C52-Na1-C12-N11	-146.82(7)	C32-Na1-C22-C12	-126.87(9)
C62#3-Na1-C12-N11	126.75(8)	C32#3-Na1-C22-C12	-99.66(6)
C62-Na1-C12-N11	-115.85(9)	C22#3-Na1-C22-C12	-110.15(5)
C42-Na1-C12-N11	179.56(7)	S1-Na1-C22-C72	-46.48(7)
C42#3-Na1-C12-N11	-166.97(6)	C52#3-Na1-C22-C72	94.52(8)
C12#3-Na1-C12-N11	6.24(6)	C52-Na1-C22-C72	179.05(8)
C32-Na1-C12-N11	147.34(8)	C62#3-Na1-C22-C72	68.38(8)
C32#3-Na1-C12-N11	-134.24(6)	C62-Na1-C22-C72	-146.73(9)
C22#3-Na1-C12-N11	-104.07(9)	C42-Na1-C22-C72	145.39(9)
C62-C12-C22-C32	2.73(13)	C42#3-Na1-C22-C72	123.97(7)
N11-C12-C22-C32	-174.16(8)	C12-Na1-C22-C72	-116.33(10)
Na1-C12-C22-C32	-61.82(8)	C12#3-Na1-C22-C72	61.64(11)
C62-C12-C22-C72	-176.65(8)	C32-Na1-C22-C72	116.80(10)
N11-C12-C22-C72	6.46(13)	C32#3-Na1-C22-C72	144.00(7)
Na1-C12-C22-C72	118.80(9)	C22#3-Na1-C22-C72	133.52(7)
C62-C12-C22-Na1	64.55(7)	C12-C22-C32-C42	-1.21(15)

C72-C22-C32-C42	178.18(9)	C32#3-Na1-C42-C32	150.71(5)
Na1-C22-C32-C42	-61.72(9)	C22#3-Na1-C42-C32	147.53(6)
C12-C22-C32-Na1	60.51(8)	S1-Na1-C42-C52	75.88(8)
C72-C22-C32-Na1	-120.10(9)	C52#3-Na1-C42-C52	-131.33(6)
S1-Na1-C32-C42	148.40(5)	C62#3-Na1-C42-C52	-138.05(6)
C52#3-Na1-C32-C42	-72.64(6)	C62-Na1-C42-C52	30.25(6)
C52-Na1-C32-C42	30.81(6)	C42#3-Na1-C42-C52	-104.12(8)
C62#3-Na1-C32-C42	-90.88(6)	C12-Na1-C42-C52	64.11(6)
C62-Na1-C32-C42	64.94(6)	C12#3-Na1-C42-C52	-116.03(6)
C42#3-Na1-C32-C42	-45.20(7)	C32-Na1-C42-C52	124.99(9)
C12-Na1-C32-C42	98.77(7)	C32#3-Na1-C42-C52	-84.30(6)
C12#3-Na1-C32-C42	-82.07(7)	C22#3-Na1-C42-C52	-87.48(6)
C32#3-Na1-C32-C42	-31.60(5)	C32-C42-C52-C62	0.51(16)
C22#3-Na1-C32-C42	-44.18(7)	Na1-C42-C52-C62	-67.76(9)
S1-Na1-C32-C22	20.14(7)	C32-C42-C52-Na1	68.27(9)
C52#3-Na1-C32-C22	159.09(7)	S1-Na1-C52-C42	-132.20(5)
C52-Na1-C32-C22	-97.45(7)	C52#3-Na1-C52-C42	47.80(5)
C62#3-Na1-C32-C22	140.86(6)	C62#3-Na1-C52-C42	51.47(7)
C62-Na1-C32-C22	-63.32(6)	C62-Na1-C52-C42	-125.72(10)
C42-Na1-C32-C22	-128.26(9)	C42#3-Na1-C52-C42	68.24(8)
C42#3-Na1-C32-C22	-173.46(6)	C12-Na1-C52-C42	-94.96(7)
C12-Na1-C32-C22	-29.49(5)	C12#3-Na1-C52-C42	85.64(7)
C12#3-Na1-C32-C22	149.67(6)	C32-Na1-C52-C42	-29.82(6)
C32#3-Na1-C32-C22	-159.86(7)	C32#3-Na1-C52-C42	94.15(7)
C22#3-Na1-C32-C22	-172.44(3)	C22#3-Na1-C52-C42	103.88(7)
C22-C32-C42-C52	-0.41(16)	S1-Na1-C52-C62	-6.48(7)
Na1-C32-C42-C52	-64.74(9)	C52#3-Na1-C52-C62	173.52(7)
C22-C32-C42-Na1	64.33(9)	C62#3-Na1-C52-C62	177.19(3)
S1-Na1-C42-C32	-49.11(8)	C42-Na1-C52-C62	125.72(10)
C52#3-Na1-C42-C32	103.68(6)	C42#3-Na1-C52-C62	-166.03(7)
C52-Na1-C42-C32	-124.99(9)	C12-Na1-C52-C62	30.76(5)
C62#3-Na1-C42-C32	96.96(6)	C12#3-Na1-C52-C62	-148.64(6)
C62-Na1-C42-C32	-94.74(6)	C32-Na1-C52-C62	95.90(7)
C42#3-Na1-C42-C32	130.89(8)	C32#3-Na1-C52-C62	-140.13(7)
C12-Na1-C42-C32	-60.88(6)	C22#3-Na1-C52-C62	-130.40(6)
C12#3-Na1-C42-C32	118.98(6)	C42-C52-C62-C12	1.00(14)

Na1-C52-C62-C12	-67.52(8)	C32-Na1-C62-C12	61.73(6)
C42-C52-C62-C102	-178.84(9)	C32#3-Na1-C62-C12	166.16(5)
Na1-C52-C62-C102	112.64(9)	C22#3-Na1-C62-C12	-173.52(5)
C42-C52-C62-Na1	68.52(9)	S1-Na1-C62-C102	57.88(7)
C22-C12-C62-C52	-2.63(13)	C52#3-Na1-C62-C102	-124.95(6)
N11-C12-C62-C52	174.26(8)	C52-Na1-C62-C102	-117.13(10)
Na1-C12-C62-C52	65.41(8)	C62#3-Na1-C62-C102	-122.12(7)
C22-C12-C62-C102	177.21(8)	C42-Na1-C62-C102	-147.01(8)
N11-C12-C62-C102	-5.90(13)	C42#3-Na1-C62-C102	-102.94(7)
Na1-C12-C62-C102	-114.75(9)	C12-Na1-C62-C102	118.61(9)
C22-C12-C62-Na1	-68.04(8)	C12#3-Na1-C62-C102	-59.57(10)
N11-C12-C62-Na1	108.85(7)	C32-Na1-C62-C102	-179.66(8)
S1-Na1-C62-C52	175.01(6)	C32#3-Na1-C62-C102	-75.23(7)
C52#3-Na1-C62-C52	-7.81(9)	C22#3-Na1-C62-C102	-54.91(8)
C62#3-Na1-C62-C52	-4.99(6)	C32-C22-C72-C82	68.63(13)
C42-Na1-C62-C52	-29.87(6)	C12-C22-C72-C82	-112.00(11)
C42#3-Na1-C62-C52	14.20(7)	Na1-C22-C72-C82	-23.08(12)
C12-Na1-C62-C52	-124.25(9)	C32-C22-C72-C92	-54.75(13)
C12#3-Na1-C62-C52	57.56(10)	C12-C22-C72-C92	124.62(11)
C32-Na1-C62-C52	-62.53(6)	Na1-C22-C72-C92	-146.46(8)
C32#3-Na1-C62-C52	41.91(7)	C52-C62-C102-C122	50.38(13)
C22#3-Na1-C62-C52	62.23(7)	C12-C62-C102-C122	-129.46(9)
S1-Na1-C62-C12	-60.73(5)	Na1-C62-C102-C122	138.05(7)
C52#3-Na1-C62-C12	116.44(5)	C52-C62-C102-C112	-74.07(12)
C52-Na1-C62-C12	124.25(9)	C12-C62-C102-C112	106.09(10)
C62#3-Na1-C62-C12	119.27(5)	Na1-C62-C102-C112	13.61(10)
C42-Na1-C62-C12	94.38(6)	C14-C24-C34-C44	-178.7(10)
C42#3-Na1-C62-C12	138.45(5)	C24-C34-C44-C54	-174.4(12)
C12#3-Na1-C62-C12	-178.19(7)		

Symmetry transformations used to generate equivalent atoms:

#1 x,-y,z #2 -x+2,-y,-z #3 -x+2,y,-z